Pricing bounds and approximations for discrete arithmetic Asian options under time-changed Lévy processes

Pingping Zeng
Department of Mathematics,
University of Vienna, Austria

Yue Kuen Kwok[1]
Department of Mathematics,
Hong Kong University of Science and Technology, Hong Kong

October, 2015

Abstract
We derive efficient and accurate analytical pricing bounds and approximations for discrete arithmetic Asian options under time-changed Lévy processes. By extending the conditioning variable approach, we derive the lower bound on the Asian option price and construct an upper bound based on the sharp lower bound. We also consider the general partially exact and bounded (PEB) approximations, which include the sharp lower bound and partially conditional moments matching approximation as special cases. The PEB approximations are known to lie between a sharp lower bound and an upper bound. Our numerical tests show that the PEB approximations to discrete arithmetic Asian option prices can produce highly accurate approximations when compared to other approximation methods. Our proposed approximation methods can be readily applied to pricing Asian options under most common types of underlying asset price processes, like the Heston stochastic volatility model nested in the class of time-changed Lévy processes with the leverage effect.

Keywords: time-changed Lévy processes, arithmetic Asian options, conditioning variable approach, partially exact and bounded approximations

1 Introduction

Under the assumption of Geometric Brownian motion for the underlying asset process, it is known that there is no closed form solution for the discrete arithmetic Asian option since there is no explicit analytical expression available for the distribution of the arithmetic average (expressed as a sum of correlated lognormal random variables). There have been continual research efforts in the past two decades to explore effective analytical and numerical approaches for pricing arithmetic Asian options. One common approach is the dimension reduction of the pricing model that reduces the governing two-dimensional partial differential equation to its degenerate one-dimensional form by including the path dependent variable into the state space (Rogers and Shi, 1995; Vecer, 2001). Geman and Yor (1993) use the Laplace transform to derive a closed form expression for a continuous arithmetic Asian option in the Laplace transform domain. Benhamou (2002) proposes the fast Fourier transform algorithm for pricing discrete arithmetic Asian option, which is an enhanced version of the convolution algorithm of Carverhill and Clewlow (1990) that decomposes the arithmetic average into a product of independent random variables. Curran (1992, 1994) and Rogers

[1]Correspondence author; email: maykwok@ust.hk; fax number: 852-2358-1643

and Shi (1995) manage to derive a lower bound by using the conditioning variable approach together with the application of Jensen's inequality. Rogers and Shi (1995) also derive an upper bound via an estimation of the error based on the lower bound under continuous arithmetic averaging. The upper bound is later sharpened by Nielsen and Sandmann (2003) considerably. Simon *et al.* (2000) propose the comonotonic upper bound (CUB) using some results from risk theory on stop-loss order. Later, Vanmaele *et al.* (2006) improve on the CUB by the conditioning variable approach and also propose the partially exact CUB. Besides these various versions of the conditioning variable approach, there are several works that explore different analytical approximations based on the method of matching moments. Levy (1992) finds the closed form analytical approximation by assuming a given form for the density of the arithmetic average. Turnbull and Wakeman (1991) approximate the density using an Edgeworth series expansion around a lognormal density based on the first four algebraic moments of the arithmetic average. Lord (2006a) introduces the partially exact and bounded (PEB) approximations, which combine the conditioning variable approach and conditional moment matching approach. Common numerical methods for pricing Asian options include the Monte Carlo simulation, binomial trees method (Hull and White, 1993) and finite difference method (Andreasen, 1998). A more comprehensive review of the literature on pricing arithmetic Asian options under the Geometric Brownian motion for the underlying price process can be found in Lord (2006a).

When it comes to pricing Asian options under Lévy processes, the literature is relatively thin compared to that of the Geometric Brownian motion model. Fusai and Meucci (2008) apply numerical quadrature in a recursive integration algorithm for computing the convolution of density functions over successive monitoring dates. Zhang and Oosterlee (2013) combine the Fourier cosine expansions and Clenshaw-Curtis quadrature method for discretely and continuously monitored arithmetic Asian options. Instead of calculating the density functions in a recursive manner as in Fusai and Meucci (2008), they recover the characteristic function by means of the Fourier cosine expansions. Fusai *et al.* (2011) extend the methodology based on maturity randomization to the pricing of Asian options. The comonotonic upper bounds are developed by Albrecher *et al.* (2005) under Lévy models. Lemmens *et al.* (2010) derive bounds for discrete arithmetic Asian options under a general Lévy model based on the conditioning variable approach similar to the bounds under the Geometric Brownian motion model (Rogers and Shi, 1995; Nielsen and Sandmann 2003). Lord (2006b) studies the lower pricing bounds for basket options in a setting where the characteristic function of the underlying price process is known. The innovative techniques are then applied to derive approximation formulas for swaptions and Asian options in affine Lévy models. Albrecher *et al.* (2008) give arbitrage-free model independent lower bounds for arithmetic Asian option prices. Some of their bounds are supposed to hold across every arbitrage-free model, but the corresponding accuracy levels are worse than those approximations obtained by specifying a particular model.

Since Lévy processes cannot capture the following salient features of common stock price processes: stochastic volatility, stochastic risk reversal (skewness) and stochastic correlation, Carr and Wu (2004) propose the time-changed Lévy processes that nest some popular stochastic volatility models. Since the time-changed Lévy processes are more complex and do not have the independent increments property, the corresponding pricing of Asian options under time-changed Lévy processes poses high level of mathematical challenge. Umezawa and Yamazaki (2015) derive the multivariate characteristic functions of the intertemporal joint distribution of time-changed Lévy processes and use them to find semi-analytical pricing formula for geometric Asian options. Yamazaki (2014) prices continuous and discrete arithmetic Asian options by applying the Gram-Charlier expansion to find analytic approximation formulas based on the moments of the arithmetic average asset price under time-changed Lévy processes. This is regarded as the generalized Edgeworth expansion around the Gaussian distribution, which provides approximations of the density function of an arbitrary random variable. However, the Edgeworth approximation results may converge for a small number of terms in moment matching but diverge for a larger number of terms.

In this paper, we first derive the same sharp lower bound of the discrete arithmetic Asian option price using different methods based on the conditioning variable technique of Curran (1994). In one of these methods, we generalize the method of Lemmens *et al.* (2010) by extending from Lévy models to time-changed Lévy processes. Next, we construct an upper bound based on the sharp lower bound by following a similar technique proposed by Nielsen and Sandmann (2003). Finally, we consider the class of the partially exact and bounded (PEB) approximations similar to those introduced by Lord (2006a) under the Geometric Brownian motion model. Unlike the traditional moment matching approach, the PEB approximations are proven to lie between a sharp lower and an upper bound. Moreover, when the strike price approaches to zero or infinity, the PEB approximations converge to the exact Asian option price. We manage to derive analytic approximation formulas using the explicit analytic forms of the multivariate characteristic functions of the intertemporal joint distribution of time-changed Lévy processes (Umezawa and Yamazaki, 2015). Our numerical tests demonstrate high level of accuracy, efficiency and reliability of the PEB approximations when compared to other approximation methods in the literature.

The paper is organized as follows. Section 2 introduces some mathematical preliminaries on time-changed Lévy processes and the associated multivariate characteristic functions of the intertemporal joint distribution. In Section 3, we show how to decompose the price of an Asian option into two components based on the conditioning variable approach. The major component can be evaluated to give an exact analytical formula while the residual component is evaluated using analytic bounds and approximations. In Section 4, we derive the lower and upper pricing bounds of the discrete arithmetic Asian option. We also propose the class of the partially exact and bounded approximations to approximate the residual component in the decomposition formula. Specifically, we adopt the method of the partial conditional moment matching in the deviation. Section 5 presents the explicit analytic form of the associated multivariate characteristic functions of the intertemporal joint distribution of time-changed Lévy processes. In Section 6, we present the numerical tests that were performed to assess accuracy and computational efficiency of various methods that produce bounds and approximations under different time-changed Lévy processes. Conclusive remarks are presented in the last section.

2 Preliminaries on time-changed Lévy processes

The literature on Lévy processes has been quite voluminous. A good review of various Lévy security return models can be found in Wu (2008). Pricing models of financial derivatives based on Lévy processes have been highly popular in recent years since Lévy processes can generate different independent and identically (i.i.d) return innovation distributions. One can specify a Lévy process with the increments of the process matching any given distribution. To capture stochastic volatility, we can apply a stochastic time change to the Lévy process. We are also able to capture the correlation by letting the Lévy process be correlated with the activity rate which generates the corresponding time change. Therefore, time-changed Lévy processes provide a flexible framework for generating jumps, capturing stochastic volatility and introducing the leverage effect. Pricing of options under time-changed Lévy processes also enjoys nice analytical tractability.

In fact, since the pioneering work of Clark (1973) that shows how a random time change can be interpreted as a cumulative measure of business activity, time-changed Lévy processes have already seen a wide range of applications in option pricing theory. In particular, Carr and Wu (2004) provide a framework for option pricing under time-changed Lévy processes that encompasses almost all of the models proposed in the option pricing literature. There is also a growing literature on applying time-changed Lévy processes for pricing other types of path dependent options and variance products (Umezawa and Yamazaki, 2015; Itkin and Carr, 2010).

2.1 Time-changed Lévy processes

Under an equivalent martingale measure Q, the Lévy-Khintchine theorem postulates that a general Lévy process X_t has its characteristic function represented in the following analytic form

$$\phi_t(\xi) = E_Q[e^{i\xi X_t}] = e^{-t\psi_X(\xi)} = \exp\bigg(-t\Big[\frac{\sigma^2}{2}\xi^2 - i\mu\xi + \int_R (1 - e^{i\xi y} + i\xi y \mathbf{1}_{|y|\le 1})\,\Pi(dy)\Big]\bigg), \quad (2.1)$$

where the triplet (μ, σ^2, Π) characterizes the drift, the variance of the diffusion component, and the pure jump component of a Lévy process; and $\psi_X(\xi)$ is known as the Lévy characteristic exponent. We let T_t be a non-negative, non-decreasing right-continuous process with left limits. For each fixed t, the random variable T_t is a stopping time with respect to the filtration $\mathcal{F}_t$. The family of the stopping times T_t define the corresponding random time change and the resulting process

$$M_t = X_{T_t} \quad (2.2)$$

is called a time-changed Lévy process and X_t is referred as the base process. The two procedures for generating the Lévy process that captures any distribution and the time change that captures the stochastic volatility can be separated. There are different methods for choosing time changes that are appropriate for various types of financial security return models. The two most popular approaches are the subordinators and absolutely continuous time changes (Zeng and Kwok, 2014).

In this paper, we assume that the random time changes are given by the continuous time change of the form

$$T_t = \int_0^t v_s \,\mathrm{d}s, \quad (2.3)$$

where v_t is the instantaneous (business) activity rate. We model the dynamics of the underlying log-asset return by a time-changed Lévy process of the following form

$$S_t = S_0 e^{(r-q)t + X_{T_t} + \varpi_t}, \quad (2.4)$$

where r and q denote the constant risk free interest rate and dividend yield, respectively, and ϖ_t is an appropriate process to be chosen in order that $e^{X_{T_t}+\varpi_t}$ is a martingale under Q. By the optional stopping theorem, $e^{X_{T_t}+\psi_X(-i)T_t}$ is a martingale. It follows that $\varpi_t = \psi_X(-i)T_t$; and we write

$$Z_t = X_{T_t} + \psi_X(-i)T_t.$$

As a result, Z_t is related to S_t by the following formula

$$S_t = S_0 e^{(r-q)t + Z_t}. \quad (2.5)$$

2.2 Multivariate characteristic functions

Umezawa and Yamazaki (2015) derive an explicit analytic form of the multivariate characteristic function of the intertemporal joint distribution of time-changed Lévy processes. We provide a brief summary of their main results that are relevant to this paper.

The characteristic function of a time-changed Lévy process can be calculated by changing measures as follows (Carr and Wu, 2004):

$$\phi_{X_{T_t}}(\theta) = E_Q[e^{i\theta X_{T_t}}] = E^{(\theta)}[e^{-\psi_X(\theta)T_t}], \tag{2.6}$$

where E_Q and $E^{(\theta)}$ denote the expectation under a risk neutral measure Q and a new complex-valued measure $Q(\theta)$, respectively. The measure $Q(\theta)$ is absolutely continuous with respect to the risk neutral measure Q and it is defined by

$$\mathbb{M}_t(\theta) = \frac{\mathrm{d}\mathbb{Q}(\theta)}{\mathrm{d}\mathbb{Q}}|_t = e^{i\theta X_{T_t} + T_t \psi_X(\theta)}. \tag{2.7}$$

Here, $\mathbb{M}_t(\theta)$ is a complex-valued exponential martingale by virtue of the optional stopping theorem. By changing the measure from Q to $Q(\theta)$, the correlation between X_t and v_t is hidden under the new complex measure $Q(\theta)$. Suppose the base Lévy process X_t of a time-changed Lévy process X_{T_t} is independent of its time change process T_t, the characteristic function of the time changed Lévy process X_{T_t} is the Laplace transform of T_t evaluated at the characteristic exponent of X without changing measures, where

$$\phi_{X_{T_t}}(\theta) = E[e^{-\psi_X(\theta)T_t}].$$

We consider the multivariate characteristic function of the intertemporal joint distribution of $Z = (Z_{t_1}, Z_{t_2}, \cdots, Z_{t_N})^{\mathrm{T}}$, where $0 \leq t_1 \leq t_2 \leq \cdots t_N \leq T$; and write

$$\phi_Z(\Theta) = E[e^{i\Theta^T Z}], \tag{2.8}$$

where $\Theta = (\theta_1, \cdots, \theta_N)^{\mathrm{T}}$ is a parameter vector of the characteristic function on $\mathbb{R}^N$. The representation of the multivariate characteristic function of the intertemporal joint distribution can be obtained in the form of a recursive conditional expectation (Umezawa and Yamazaki, 2015) as stated in Proposition 1.

Proposition 1 *Let $(I_j)_{1\leq j\leq N}$ be a backward relation such that*

$$I_{j-1} = E^{(\sum_{k=j}^N \theta_k)}\left[e^{-\kappa_j \int_{t_{j-1}}^{t_j} v_s \,\mathrm{d}s} I_j | \mathcal{F}_{t_{j-1}}\right], \tag{2.9}$$

where $I_N = 1$, and

$$\kappa_j = \psi_X\left(\sum_{k=j}^N \theta_k\right) - i\left(\sum_{k=j}^N \theta_k\right)\psi_X(-i).$$

The multivariate characteristic function of the intertemporal joint distribution of Z is given by

$$\phi_Z(\Theta) = I_0. \tag{2.10}$$

Corollary 1 *Suppose the base Lévy process X_t of a time-changed Lévy process X_{T_t} is independent of its time change process T_t, then we have*

$$\phi_Z(\Theta) = E\left[e^{-\sum_{j=1}^N \kappa_j \int_{t_{j-1}}^{t_j} v_s \,\mathrm{d}s}\right]. \tag{2.11}$$

Based on the result in Proposition 1, we derive various analytic forms of the multivariate characteristic function of the intertemporal joint distribution for some specific activity rate processes. The details are shown in Section 5.

3 Decomposition of the arithmetic Asian option price via conditioning approach

Considering a European discrete arithmetic Asian call option on an underlying asset S_t with $N+1$ monitoring dates and fixed strike price K, its terminal payoff at maturity T is given by

$$\left(\frac{1}{N+1}\sum_{k=0}^{N} S_{t_k} - K\right)^+. \tag{3.1}$$

Here, we let the current time be $t_0 = 0$, and denote the set of monitoring times for the Asian option by $\mathcal{T} = \{t_0, t_1, \cdots, t_N\}$, where $t_N = T$. Though the time intervals between successive monitoring times may not be uniform in general, without loss of generality, we assume a uniform monitoring interval Δ to simplify the presentation. For uniform time intervals, we have $t_k = k\Delta,\ k = 0, 1, \cdots, N$. In terms of the arithmetic average as defined by

$$A_T = \frac{1}{N+1}\sum_{k=0}^{N} S_{t_k},$$

the risk neutral price of the discrete arithmetic Asian call option at the current time $t = 0$ is given by

$$C_A(T,K) = e^{-rT}E_Q[(A_T - K)^+], \tag{3.2}$$

where E_Q denotes the expectation under a risk neutral measure Q. Later, we drop the subscript "Q" in the expectation operator E_Q for brevity. Recall that $S_t = S_0e^{(r-q)t+Z_t}$ [see Eq. (2.5)] and $Z_0 = 0$, the discrete arithmetic average of Z_t is denoted by

$$\bar{Z}_T = \frac{1}{N+1}\sum_{k=1}^{N} Z_{t_k}. \tag{3.3}$$

For notational convenience, we write S_{t_k} and Z_{t_k} as S_k and Z_k, respectively.

We consider the decomposition of the Asian call option value into two components via conditioning on a random variable Λ (Curran, 1994). It is desirable to choose the conditioning variable Λ such that there is a threshold value $\lambda(K)$ for which $\Lambda \geq \lambda(K)$ implying $A_T \geq K$. Conditioning on Λ, the above property allows one to split the expectation for the Asian call option value into two components as follows

$$C_A(T,K) = e^{-rT}E[(A_T - K)^+\mathbf{1}_{\{\Lambda<\lambda(K)\}}] + e^{-rT}E[(A_T - K)\mathbf{1}_{\{\Lambda\geq\lambda(K)\}}]. \tag{3.4}$$

The optionality on $A_T - K$ disappears in the second term since $\Lambda \geq \lambda(K)$ would imply $A_T \geq K$. We use $C_1(T,K,\Lambda,\lambda(K))$ and $C_2(T,K,\Lambda,\lambda(K))$ to denote the above two expectation terms, respectively. If we choose a proper conditioning variable Λ, a significant percentage of the value of the Asian option can be evaluated exactly in closed form, so it is termed the "exact" component. The residual component has a small contribution to the Asian option value, which is then estimated via some analytic bounds or approximation technique. The details of the above procedures are presented in the subsequent sections.

To minimize pricing error of the approximation, it is desirable to choose the conditioning variable Λ that is strongly correlated to A_T. This leads to the smaller contribution of $C_1(T,K,\Lambda,\lambda(K))$ to the Asian option price. In the most ideal scenario, the perfect correlation between A_T and Λ would result in zero pricing error. A good choice for the conditioning variable is the geometric average since the geometric and arithmetic averages are strongly correlated. We write

$$G_T = (S_0S_1\cdots S_N)^{\frac{1}{N+1}} = e^{\ln S_0 + \frac{r-q}{2}T + \bar{Z}_T}.$$

Here, it is appropriate to choose $\bar{Z}_T$ as the conditioning variable for convenience. The corresponding threshold is given by

$$\lambda(K) = \ln \frac{K}{S_0} + \frac{q-r}{2}T.$$

Without optionality in the payoff, the second component $C_2(T, K, \Lambda, \lambda(K))$ can be evaluated analytically. Using the tower property, we have

$$\begin{aligned} C_2(T, K, \Lambda, \lambda(K)) &= e^{-rT} E\left[E[(A_T - K)\mathbf{1}_{\{\Lambda \geq \lambda(K)\}}|\Lambda]\right] \\ &= e^{-rT} E\left[(E[A_T|\Lambda] - K)\,\mathbf{1}_{\{\Lambda \geq \lambda(K)\}}\right]. \end{aligned} \tag{3.5}$$

The outer expectation over Λ can be expressed as

$$C_2(T, K, \Lambda, \lambda(K)) = e^{-rT} \int_{-\infty}^{\infty} (E[A_T|\Lambda = \lambda] - K)\,\mathbf{1}_{\{\lambda \geq \lambda(K)\}} f_\Lambda(\lambda)\ \mathrm{d}\lambda, \tag{3.6}$$

where $f_\Lambda(\lambda)$ is the density function of Λ.

We consider the generalized Fourier transform of the indicator function $\mathbf{1}_{\{\lambda > \lambda(K)\}}$, visualized as a function of λ, where

$$\int_{-\infty}^{\infty} \mathbf{1}_{\{\lambda > \lambda(K)\}} e^{-i\omega\lambda}\ \mathrm{d}\lambda = \frac{e^{-i\omega\lambda(K)}}{i\omega}.$$

Here, $\omega = \omega_R + i\omega_I$ and ω_I is a negative scalar that is appropriately chosen to guarantee that the above generalized Fourier transform exists. By taking the corresponding generalized inverse Fourier transform, we obtain

$$\mathbf{1}_{\{\lambda > \lambda(K)\}} = \frac{1}{2\pi} \int_{-\infty}^{\infty} e^{i\omega\lambda} \frac{e^{-i\omega\lambda(K)}}{i\omega}\ \mathrm{d}\omega_R.$$

The above analytic representation of the indicator function in terms of a generalized inverse Fourier integral is substituted into Eq. (3.6). By interchanging the order of integration, we manage to obtain

$$\begin{aligned} C_2(T, K, \Lambda, \lambda(K)) &= \frac{e^{-rT}}{2\pi} \int_{-\infty}^{\infty} \frac{e^{-i\omega\lambda(K)}}{i\omega} \int_{-\infty}^{\infty} (E[A_T|\Lambda = \lambda] - K)\, e^{i\omega\lambda} f_\Lambda(\lambda)\ \mathrm{d}\lambda \mathrm{d}\omega_R \\ &= \frac{e^{-rT}}{2\pi} \int_{-\infty}^{\infty} \frac{e^{-i\omega\lambda(K)}}{i\omega} \left(E[A_T e^{i\omega\Lambda}] - KE[e^{i\omega\Lambda}]\right)\ \mathrm{d}\omega_R. \end{aligned} \tag{3.7}$$

Let $\phi_\Lambda(\omega)$ denote the characteristic function of the conditioning variable Λ and $\phi_{\Lambda, Z_k}(\omega_1, \omega_2)$ denote the joint characteristic function of Λ and Z_k. By defining

$$\hat{g}(\omega) = E[A_T e^{i\omega\Lambda}] - KE[e^{i\omega\Lambda}],$$

it then follows that

$$\hat{g}(\omega) = \frac{S_0}{N+1}\left[\phi_\Lambda(\omega) + \sum_{k=1}^{N} e^{(r-q)k\Delta} \phi_{\Lambda, Z_k}(\omega, -i)\right] - K\phi_\Lambda(\omega). \tag{3.8}$$

With the choice $\Lambda = \bar{Z}_T$, it follows that $\phi_\Lambda(\omega) = \phi_Z(\Theta^{(1)})$, where the j^{th} component of $\Theta^{(1)}$ is given by $\theta_j^{(1)} = \frac{\omega}{N+1}$, $j = 1, 2, \cdots, N$. Note that $\phi_{\Lambda, Z_k}(\omega, -i) = \phi_Z(\Theta^{(2)})$, where the components of $\Theta^{(2)}$ are given by $\theta_j^{(2)} = \frac{\omega}{N+1}$ for any $j \neq k$, and $\theta_k^{(2)} = \frac{\omega}{N+1} - i$. As a result, $C_2(T, K, \Lambda, \lambda(K))$ can be simplified to become a single Fourier integral as follows

$$C_2(T, K, \Lambda, \lambda(K)) = -\frac{e^{-rT} i}{2\pi} \int_{-\infty}^{\infty} \frac{e^{-i\omega\lambda(K)} \hat{g}(\omega)}{\omega}\ \mathrm{d}\omega_R. \tag{3.9}$$

4 Analytic pricing bounds and approximations

In this section, we first discuss various approaches that give bounds for the residual component $C_1(T,K,\Lambda,\lambda(K))$. Next, we propose the partially exact and bounded approximations by adopting the method of the partial conditional moments matching.

4.1 Lower bounds

Observe that $C_1(T,K,\Lambda,\lambda(K))$ is bounded below by

$$\begin{aligned} C_1(T,K,\Lambda,\lambda(K)) &= e^{-rT}E[(A_T-K)^+\mathbf{1}_{\{\Lambda<\lambda(K)\}}] \\ &\geq e^{-rT}E\left[(A_T-K)\mathbf{1}_{\{l<\Lambda<\lambda(K)\}}\right] \end{aligned} \tag{4.1}$$

for any l. Here, we choose a new event set $\mathbf{1}_{\{l<\Lambda<\lambda(K)\}}$ that is a close proxy to the true event set $\mathbf{1}_{\{A_T>K\}\cap\{\Lambda<\lambda(K)\}}$ by optimizing over l while making the problem more analytically tractable. By adding the "exact" component $C_2(T,K,\Lambda,\lambda(K))$ to an approximation of $C_1(T,K,\Lambda,\lambda(K))$, we obtain the following lower bound for the discrete arithmetic Asian call option price

$$C_A(T,K) \geq e^{-rT}E\left[(A_T-K)\mathbf{1}_{\{\Lambda>l\}}\right]. \tag{4.2}$$

In fact, the above inequality holds for any random variable Λ. We write

$$LB_l(\Lambda) = e^{-rT}E\left[(A_T-K)\mathbf{1}_{\{\Lambda>l\}}\right],$$

then the lower bound can be evaluated in a similar manner as the "exact" component by virtue of the following relation

$$LB_l(\Lambda) = C_2(T,K,\Lambda,l).$$

We consider the differentiation of $LB_l(\Lambda)$ with respect to the parameter l and obtain

$$\frac{\mathrm{d}LB_l(\Lambda)}{\mathrm{d}l} = -\frac{e^{-rT}}{2\pi}\int_{-\infty}^{\infty} e^{-i\omega l}\hat{g}(\omega)\ \mathrm{d}\omega_R,$$

where $\hat{g}(\omega)$ is defined in Eq. (3.8). In addition, it is seen that $LB_l(\Lambda)$ does not achieve its maximum when l is sufficiently small and $LB_l(\Lambda)$ is a decreasing function when $l \in [\lambda(K),\infty)$. As a result, the sharp lower bound achieved under the form of inequality (4.2) is seen to be

$$LB(\Lambda) = \max_{l\leq\lambda(K)} LB_l(\Lambda) = -\frac{e^{-rT}i}{2\pi}\int_{-\infty}^{\infty}\frac{e^{-i\omega\lambda^*}\hat{g}(\omega)}{\omega}\ \mathrm{d}\omega_R, \tag{4.3}$$

where the optimal choice $\lambda^* \leq \lambda(K)$ satisfies the following first order condition

$$-\frac{e^{-rT}}{2\pi}\int_{-\infty}^{\infty} e^{-i\omega x}\left[\frac{S_0}{N+1}\left(\phi_\Lambda(\omega)+\sum_{k=1}^{N}e^{(r-q)k\Delta}\phi_{\Lambda,Z_k}(\omega,-i)\right)-K\phi_\Lambda(\omega)\right]\ \mathrm{d}\omega_R = 0. \tag{4.4}$$

One can resort to the Newton-Raphson method with the initial guess $\lambda=\lambda(K)$ to solve Eq. (4.4). One should check for the second order condition $\frac{\mathrm{d}^2LB_l(\Lambda)}{\mathrm{d}l^2}\leq 0$ as well to ensure that λ^* is a maximizer of the function $LB_l(\Lambda)$. If the maximizer is not unique, we adopt λ^* to denote the smallest one.

The procedure for finding the sharp lower bound is summarized in Theorem 1.

Theorem 1 *A sharp lower bound of the discrete arithmetic Asian option price admits the following analytic representation*

$$LB(\Lambda) = \; -\frac{e^{-rT}i}{2\pi}\int_{-\infty}^{\infty}\frac{e^{-i\omega\lambda^*}\hat{g}(\omega)}{\omega}\,\mathrm{d}\omega_R, \tag{4.5}$$

where $\hat{g}(\omega)$ is defined in Eq. (3.8) and λ^* is obtained from Eq. (4.4).

Remarks

1. Since this analytic lower bound for the Asian option price has been very tight and can be evaluated at ease, it is not quite necessary to consider optimizing over the choices of the conditioning variable Λ. In Section 6, we show that the geometric average is a better conditioning variable compared to S_t for any $0 \le t \le T$. Here, the threshold $\lambda(K)$ serves as a technical tool for making the link between the "exact" component and the residual component, and does not appear in the final expression (4.5) for the lower bound. However, the upper bound and other approximations do depend on the threshold $\lambda(K)$ (see later discussion).

2. The Envelope Theorem states that the derivative of the optimizer of the objective function with respect to the parameter equals the partial derivative of the objective function with respect to this parameter holding the maximizer fixed at its optimal level. An application of the Envelope Theorem gives the partial derivative of the lower bound with respect to the initial asset as follows

$$\frac{\partial LB(\Lambda)}{\partial S_0} = \; -\frac{e^{-rT}i}{2\pi}\int_{-\infty}^{\infty}\frac{e^{-i\omega\lambda^*}\left[\phi_\Lambda(\omega)+\sum_{k=1}^{N}e^{(r-q)k\Delta}\phi_{\Lambda,Z_k}(\omega,-i)\right]}{(N+1)\omega}\,\mathrm{d}\omega_R. \tag{4.6}$$

   Similar ideas have been used in Caldana and Fusai (2013) and Caldana *et al.* (2014). In fact, Eq. (4.6) provides an approximation formula for calculating the option delta of the discrete arithmetic Asian call option. However, the formula does not provide a lower bound on the option delta since the approximation error can be positive or negative.

3. Define $\mathcal{L}_X = \{\theta \in \mathrm{R} : E[e^{-\theta X_t}] < \infty, t > 0\}$, which can be shown to be an interval of the form (ζ_-, ζ_+) (Sato, 1999; Lord and Kahl, 2007). To guarantee the existence of $\phi_\Lambda(\omega)$, $\phi_{\Lambda,Z_k}(\omega,-\mathrm{i})$, and the generalized Fourier transform of the indicator function $\mathbf{1}_{\{\lambda>l\}}$ for any l, we choose $\omega_I \in (\zeta_- + 1, 0)$, where $\zeta_- < -1$. The optimal damping factor ω_I should be chosen to ensure that the integrand in the Fourier integral in Eq. (4.5) is neither peaked nor oscillatory. Interested readers are referred to Section 3 of Lord and Kahl (2007) for more details on the search of the damping factor.

Alternative lower bound

Alternatively, by means of Jensen's inequality, $C_1(T,K,\Lambda,\lambda(K))$ is bounded below by

$$\begin{aligned} C_1(T,K,\Lambda,\lambda(K)) &= e^{-rT}E[(A_T-K)^+\mathbf{1}_{\{\Lambda<\lambda(K)\}}] \\ &= e^{-rT}E\left[E[(A_T-K)^+|\Lambda]\mathbf{1}_{\{\Lambda<\lambda(K)\}}\right] \\ &\ge e^{-rT}E\left[(E[A_T|\Lambda]-K)^+\mathbf{1}_{\{\Lambda<\lambda(K)\}}\right]. \end{aligned} \tag{4.7}$$

By adding the "exact" component $C_2(T,K,\Lambda,\lambda(K))$, we obtain an alternative lower bound for the discrete arithmetic Asian call option price

$$C_A(T,K) \ge e^{-rT}E\left[(E[A_T|\Lambda]-K)^+\right]. \tag{4.8}$$

We write

$$LB2(\Lambda) = e^{-rT}E\left[(E[A_T|\Lambda] - K)^+\right] = e^{-rT}\int_{-\infty}^{\infty} (E[A_T|\Lambda = \lambda] - K)^+ f_\Lambda(\lambda)\ \mathrm{d}\lambda,$$

which is seen to be greater than or equal to $LB(\Lambda)$. Interchanging the order of the conditional expectation and summation, the conditional expectation of the arithmetic average can be represented by

$$E[A_T|\Lambda = \lambda] = \frac{S_0}{N+1}\left[1 + \sum_{k=1}^{N} e^{(r-q)k\Delta}E[e^{Z_k}|\Lambda = \lambda]\right]. \tag{4.9}$$

The individual conditional expectation can be expressed as

$$E[e^{Z_k}|\Lambda = \lambda] = \int_{-\infty}^{\infty} e^{z_k}\frac{f(\lambda, z_k)}{f_\Lambda(\lambda)}\ \mathrm{d}z_k, \quad k = 1, 2, \cdots, N, \tag{4.10a}$$

where $f(\lambda, z_k)$ is the joint probability density function for Λ and Z_k. We express the joint density function $f(\lambda, z_k)$ as the following Fourier transform representation

$$f(\lambda, z_k) = \frac{1}{4\pi^2}\int_{-\infty}^{\infty}\int_{-\infty}^{\infty} e^{-i\omega_1\lambda - i\omega_2 z_k}\phi_{\Lambda,Z_k}(\omega_1, \omega_2)\ \mathrm{d}\omega_{1R}\mathrm{d}\omega_{2R}.$$

Here, $\omega_1 = \omega_{1R} + i\omega_{1I}$ and $\omega_2 = \omega_{2R} + i\omega_{2I}$. Substituting Eq. (4.1) into Eq. (4.10a) and interchanging the order of integration, the conditional expectation $E[e^{Z_k}|\Lambda = \lambda]$ can be simplified as follows

$$\begin{aligned}
E[e^{Z_k}|\Lambda = \lambda] &= \frac{1}{4\pi^2 f_\Lambda(\lambda)}\int_{-\infty}^{\infty}\int_{-\infty}^{\infty}\int_{-\infty}^{\infty} e^{-i\omega_1\lambda - i(\omega_2+i)z_k}\phi_{\Lambda,Z_k}(\omega_1, \omega_2)\ \mathrm{d}z_k\mathrm{d}\omega_{1R}\mathrm{d}\omega_{2R} \\
&= \frac{1}{2\pi f_\Lambda(\lambda)}\int_{-\infty}^{\infty}\int_{-\infty}^{\infty} \delta(\omega_2 + i)e^{-i\omega_1\lambda}\phi_{\Lambda,Z_k}(\omega_1, \omega_2)\ \mathrm{d}\omega_{1R}\mathrm{d}\omega_{2R} \qquad (4.10\text{b}) \\
&= \frac{1}{2\pi f_\Lambda(\lambda)}\int_{-\infty}^{\infty} e^{-i\omega_1\lambda}\phi_{\Lambda,Z_k}(\omega_1, -i)\ \mathrm{d}\omega_{1R}.
\end{aligned}$$

Putting the above results into Eq. (4.9), we then obtain

$$E[A_T|\Lambda = \lambda] = \frac{S_0}{N+1}\left[1 + \frac{1}{2\pi f_\Lambda(\lambda)}\sum_{k=1}^{N} e^{(r-q)k\Delta}\int_{-\infty}^{\infty} e^{-i\omega_1\lambda}\phi_{\Lambda,Z_k}(\omega_1, -i)\ \mathrm{d}\omega_{1R}\right]. \tag{4.11}$$

Note that the density function admits a Fourier transform representation

$$f_\Lambda(\lambda) = \frac{1}{2\pi}\int_{-\infty}^{\infty} e^{-i\omega_1\lambda}\phi_\Lambda(w_1)\ \mathrm{d}\omega_{1R},$$

we then have

$$\begin{aligned}
&E[A_T|\Lambda = \lambda] - K \\
&= \frac{1}{2\pi f_\Lambda(\lambda)}\int_{-\infty}^{\infty} e^{-i\omega_1\lambda}\left\{\frac{S_0}{N+1}\left[\phi_\Lambda(\omega_1) + \sum_{k=1}^{N} e^{(r-q)k\Delta}\phi_{\Lambda,Z_k}(\omega_1, -i)\right] - K\phi_\Lambda(\omega_1)\right\}\ \mathrm{d}\omega_{1R} \\
&= -\frac{e^{rT}}{f_\Lambda(\lambda)}\frac{\mathrm{d}LB_\lambda(\Lambda)}{\mathrm{d}\lambda}. \qquad (4.12)
\end{aligned}$$

Lord (2006b) obtains an analytic result similar to Eq. (4.12) for the basket options. The crucial procedure for evaluating the lower bound $LB2(\Lambda)$ is to determine the set

$$\mathcal{S} = \{\lambda | E[A_T|\Lambda = \lambda] - K \geq 0\} = \left\{\lambda \Big| \frac{\mathrm{d}LB_\lambda(\Lambda)}{\mathrm{d}\lambda} \leq 0\right\}. \tag{4.13}$$

We would like to explore the characterization of the set $\mathcal{S}$ and examine the sufficient conditions under which equality of $LB2(\Lambda)$ and $LB(\Lambda)$ is observed. The results are summarized in Theorem 2.

Theorem 2 *Suppose the set $\mathcal{S}$ takes the form $[\tilde{\lambda}, \infty)$ for some value $\tilde{\lambda}$, we then have*

$$LB2(\Lambda) = LB(\Lambda),$$

and $\mathcal{S} = [\lambda^*, \infty)$. In addition, it suffices to observe equality of the two lower bounds when $E[A_T|\Lambda = \lambda]$ is a monotonically increasing function of λ.

Proof. Suppose the set $\mathcal{S}$ is a semi-infinite interval of the form $[\tilde{\lambda}, \infty)$ for some value $\tilde{\lambda}$, then the function $LB_\lambda(\Lambda)$ is a decreasing function of λ when $\lambda \in [\tilde{\lambda}, \infty)$, which leads to $\tilde{\lambda} \geq \lambda^*$. On the other hand, since λ^* is contained inside $\mathcal{S}$, so we have $\tilde{\lambda} \leq \lambda^*$. As a result, we obtain $\mathcal{S} = [\lambda^*, \infty)$. Based on the derived result, we manage to obtain

$$\begin{aligned} LB2(\Lambda) = &\ e^{-rT} \int_{-\infty}^{\infty} (E[A_T|\Lambda = \lambda] - K)\, \mathbf{1}_{\{\lambda > \lambda^*\}} f_\Lambda(\lambda)\, \mathrm{d}\lambda \\ &= e^{-rT} E\left[(A_T - K)\mathbf{1}_{\{\Lambda > \lambda^*\}}\right] \\ &= LB(\Lambda). \end{aligned}$$

Recall that λ^* is a root for the equation $E[A_T|\Lambda = \lambda] - K = 0$. The property of monotonically increasing of $E[A_T|\Lambda = \lambda]$ on λ immediately leads to the fact that $\mathcal{S} = [\lambda^*, \infty)$.
■

Remark
It may not be straightforward to prove rigorously whether the two sufficient conditions stated in Theorem 2 hold for all time-changed Lévy processes. At best, we manage to verify through numerical tests that some well-known time-changed Lévy processes do observe one or both of the above sufficient conditions. The details of the numerical verification are presented in Appendix A.

4.2 Upper bound based on the lower bound

To derive an upper bound based on the lower bound, we follow a similar approach in the earlier results derived under the Geometric Brownian motion framework (Rogers and Shi, 1995; Nielsen and Sandmann, 2003). According to Eq. (4.7), we can deduce an error bound to the residual component $C_1(T, K, \Lambda, \lambda(K))$ as follows

$$\begin{aligned} 0 &\leq C_1(T, K, \Lambda, \lambda(K)) - e^{-rT} E\left[(E[A_T|\Lambda] - K)^+ \mathbf{1}_{\{\Lambda < \lambda(K)\}}\right] \\ &= e^{-rT} E\left[E[(A_T - K)^+|\Lambda] \mathbf{1}_{\{\Lambda < \lambda(K)\}}\right] - e^{-rT} E\left[(E[A_T|\Lambda] - K)^+ \mathbf{1}_{\{\Lambda < \lambda(K)\}}\right] \\ &\leq \frac{e^{-rT}}{2} E\left[\sqrt{\mathrm{var}[A_T|\Lambda]}\, \mathbf{1}_{\{\Lambda < \lambda(K)\}}\right]. \end{aligned} \tag{4.14}$$

We write the above bound of the pricing error for the conditional variable approach as $\epsilon(\Lambda)$, which is seen to be model independent. By adding the "exact" component to the above inequality, it is obvious that

$$0 \leq C_A(T, K) - LB(\Lambda) \leq \epsilon(\Lambda).$$

Suppose we write $UB(\Lambda) = LB(\Lambda) + \epsilon(\Lambda)$, then $UB(\Lambda)$ can be interpreted as an upper bound based on the lower bound. Note that the bound of the pricing error $\epsilon(\Lambda)$ depends on the strike price K through $\lambda(K)$, and its value increases with the strike price. To obtain better estimation on the upper bound, Λ and A_T should be chosen to be alike as much as possible. For the ideal case that Λ and A_T are perfectly correlated, the lower bound and upper bound are equal to the exact Asian option price since the bound of the pricing error $\epsilon(\Lambda)$ is equal to zero. It is desirable to derive an easily computable analytic expression for the bound of the pricing error $\epsilon(\Lambda)$.

According to the definition of conditional variance, we have

$$\begin{aligned}\text{var}[A_T|\Lambda] = \frac{S_0^2}{(N+1)^2}\Bigg\{ & 2\sum_{k=2}^{N} e^{(r-q)k\Delta}\sum_{l=1}^{k-1} e^{(r-q)l\Delta}\left(E[e^{Z_k+Z_l}|\Lambda] - E[e^{Z_k}|\Lambda]E[e^{Z_l}|\Lambda]\right) \\ & + \sum_{k=1}^{N} e^{2(r-q)k\Delta}\left(E[e^{2Z_k}|\Lambda] - E[e^{Z_k}|\Lambda]^2\right)\Bigg\}.\end{aligned} \tag{4.15}$$

Similar to the result in Eq. (4.10b), the conditional expectations can be derived in a similar way. Assume $l < k$, these conditional expectations admit the following Fourier integral representations

$$\begin{aligned} E[e^{Z_k+Z_l}|\Lambda=\lambda] &= \frac{1}{2\pi f_\Lambda(\lambda)}\int_{-\infty}^{\infty} e^{-i\omega_1\lambda}\phi_{\Lambda,Z_k,Z_l}(\omega_1,-i,-i)\ \mathrm{d}\omega_{1R}, \\ E[e^{2Z_k}|\Lambda=\lambda] &= \frac{1}{2\pi f_\Lambda(\lambda)}\int_{-\infty}^{\infty} e^{-i\omega_1\lambda}\phi_{\Lambda,Z_k}(\omega_1,-2i)\ \mathrm{d}\omega_{1R}. \end{aligned} \tag{4.16}$$

Here, $\phi_{\Lambda,Z_k,Z_l}(\omega_1,-i,-i) = \phi_Z(\Theta^{(3)})$, where the components of $\Theta^{(3)}$ are given by $\theta_j^{(3)} = \frac{\omega_1}{N+1}$ for any $j \neq k$ and $j \neq l$, and $\theta_j^{(3)} = \frac{\omega_1}{N+1} - i$ for $j = k$ or $j = l$; and similarly, $\phi_{\Lambda,Z_k}(\omega_1,-2i) = \phi_Z(\Theta^{(4)})$, where the components of $\Theta^{(4)}$ are given by $\theta_j^{(4)} = \frac{\omega_1}{N+1}$ for any $j \neq k$, and $\theta_k^{(4)} = \frac{\omega_1}{N+1} - 2i$. Combining Eqs. (4.10b), (4.15) and (4.16), the conditional variance can be written in terms of the joint characteristic functions as follows

$$\begin{aligned} &\text{var}[A_T|\Lambda=\lambda] \\ &= \frac{S_0^2}{(N+1)^2}\Bigg\{2\sum_{k=2}^{N} e^{(r-q)k\Delta}\sum_{l=1}^{k-1} e^{(r-q)l\Delta}\Bigg[\frac{1}{2\pi f_\Lambda(\lambda)}\int_{-\infty}^{\infty} e^{-i\omega_1\lambda}\phi_{\Lambda,Z_k,Z_l}(\omega_1,-i,-i)\ \mathrm{d}\omega_{1R} \\ &\quad - \frac{1}{4\pi^2 f_\Lambda^2(\lambda)}\int_{-\infty}^{\infty} e^{-i\omega_1\lambda}\phi_{\Lambda,Z_k}(\omega_1,-i)\ \mathrm{d}\omega_{1R}\int_{-\infty}^{\infty} e^{-i\omega_1\lambda}\phi_{\Lambda,Z_l}(\omega_1,-i)\ \mathrm{d}\omega_{1R}\Bigg] \\ &\quad + \sum_{k=1}^{N} e^{2(r-q)k\Delta}\Bigg[\frac{1}{2\pi f_\Lambda(\lambda)}\int_{-\infty}^{\infty} e^{-i\omega_1\lambda}\phi_{\Lambda,Z_k}(\omega_1,-2i)\ \mathrm{d}\omega_{1R} \\ &\quad - \left(\frac{1}{2\pi f_\Lambda(\lambda)}\int_{-\infty}^{\infty} e^{-i\omega_1\lambda}\phi_{\Lambda,Z_k}(\omega_1,-i)\ \mathrm{d}\omega_{1R}\right)^2\Bigg]\Bigg\}. \end{aligned}$$

Using the Fourier transform representation of the density function $f_\Lambda(\lambda)$ and changing the order of summation and integration in the above equation, we have

$$\text{var}[A_T|\Lambda=\lambda] = \frac{S_0^2}{[(N+1)\pi f_\Lambda(\lambda)]^2}\int_{-\infty}^{\infty}\int_{-\infty}^{\infty} e^{-i(\omega_1+\omega_2)\lambda}\widetilde{g}(\omega_1,\omega_2)\ \mathrm{d}\omega_{1R}\mathrm{d}\omega_{2R}, \tag{4.17a}$$

where

$$
\begin{aligned}
\widetilde{g}(\omega_1,\omega_2) = {} & \frac{1}{2}\sum_{k=2}^{N} e^{(r-q)k\Delta}\sum_{l=1}^{k-1} e^{(r-q)l\Delta}\Big[\phi_{\Lambda,Z_k,Z_l}(\omega_1,-i,-i)\phi_\Lambda(\omega_2) - \phi_{\Lambda,Z_k}(\omega_1,-i)\phi_{\Lambda,Z_l}(\omega_2,-i)\Big] \\
& + \frac{1}{4}\sum_{k=1}^{N} e^{2(r-q)k\Delta}\Big[\phi_{\Lambda,Z_k}(\omega_1,-2i)\phi_\Lambda(\omega_2) - \phi_{\Lambda,Z_k}(\omega_1,-i)\phi_{\Lambda,Z_k}(\omega_2,-i)\Big]. \qquad (4.17\text{b})
\end{aligned}
$$

Lastly, recall that

$$
\epsilon(\Lambda) = \frac{e^{-rT}}{2}\int_{-\infty}^{\lambda(K)} \sqrt{\mathrm{var}[A_T|\Lambda=\lambda]}\; f_\Lambda(\lambda)\;\mathrm{d}\lambda.
$$

By combining all the above results, we obtain an analytic representation of the upper bound based on the lower bound as summarized in Theorem 3.

Theorem 3 *The upper bound based on the lower bound can be expressed in the following form*

$$
\begin{aligned}
UB(\Lambda) &= LB(\Lambda) + \epsilon(\Lambda) \\
&= LB(\Lambda) + \frac{e^{-rT}S_0}{2\pi(N+1)}\int_{-\infty}^{\lambda(K)} \sqrt{\int_{-\infty}^{\infty}\int_{-\infty}^{\infty} e^{-i(\omega_1+\omega_2)\lambda}\widetilde{g}(\omega_1,\omega_2)\;\mathrm{d}\omega_{1R}\mathrm{d}\omega_{2R}}\;\mathrm{d}\lambda, \qquad (4.18)
\end{aligned}
$$

where $LB(\Lambda)$ and $\widetilde{g}(\omega_1,\omega_2)$ are given by Eqs. (4.5) and (4.17b).

Remark
When the strike price K approaches to zero, and so $\lambda(K)\to-\infty$, both the lower bound and upper bound converge to the exact Asian option price. Also, the bound of the pricing error $\epsilon(\Lambda)$ increases with the strike price.

4.3 Partially exact and bounded approximations

Most analytic approximations of the arithmetic Asian option prices are based on the moment matching approach by using an analytically tractable distribution to approximate the probability law of the arithmetic average. Lord (2006a) proposes the class of partially exact and bounded (PEB) approximations for the discrete arithmetic Asian options under the Geometric Brownian motion. We would like to extend the PEB approximations to pricing arithmetic Asian options under time-changed Lévy processes.

The residual component to be approximated is given by

$$
C_1(T,K,\Lambda,\lambda(K)) = e^{-rT}E[(A_T-K)^+\mathbf{1}_{\{\Lambda<\lambda(K)\}}].
$$

The idea is to approximate A_T by $\hat{A}_T$ that is analytically tractable in the above residual component. We define

$$
\hat{C}_1(T,K,\Lambda,\lambda(K)) = e^{-rT}E[(\hat{A}_T-K)^+\mathbf{1}_{\{\Lambda<\lambda(K)\}}],
$$

and

$$
\hat{C}_A(T,K,\Lambda) = \hat{C}_1(T,K,\Lambda,\lambda(K)) + C_2(T,K,\Lambda,\lambda(K)).
$$

Applying the tower property, we have

$$
\hat{C}_1(T,K,\Lambda,\lambda(K)) = e^{-rT}E\big[E[(\hat{A}_T-K)^+|\Lambda]\mathbf{1}_{\{\Lambda<\lambda(K)\}}\big].
$$

Theorem 4 *If the approximation random variable $\hat{A}_T$ observes the following two conditions*

$$\begin{aligned} E[\hat{A}_T|\Lambda = \lambda] &= E[A_T|\Lambda = \lambda] \\ \mathrm{var}[\hat{A}_T|\Lambda = \lambda] &\leq \mathrm{var}[A_T|\Lambda = \lambda] \end{aligned} \tag{4.19}$$

for $\lambda \in (-\infty, \lambda(K))$, then $\hat{C}_A(T, K, \Lambda)$ lies between the lower bound $LB(\Lambda)$ and the upper bound $UB(\Lambda)$.

Remark
The result in Theorem 4 is model independent, so its proof can be inferred from a similar result established under the Geometric Brownian motion [see Theorem 3 of Lord (2006a)].

We refer to the class of approximations for which the above two conditions hold as the class of PEB approximations. Theorem 4 provides a sufficient condition for the PEB approximation that lies between $LB(\Lambda)$ and $UB(\Lambda)$. "Partially exact" refers to the fact that we have decomposed the option price into two components, where one of the components $C_2(T, K, \Lambda, \lambda(K))$ is obtained exactly, and "bounded" means that the PEB approximation lies between a lower and an upper bound. Indeed, one may visualize that $LB(\Lambda)$ belongs to this class of approximations, which exhibits ease of numerical evaluation and high level of accuracy.

We would like to consider some specific choices in the class of PEB approximations that match the first two conditional moments exactly, where $\lambda \in (-\infty, \lambda(K))$.

Conditional two moments matching
We consider $\hat{A}_T$ that satisfies

$$\begin{aligned} \hat{A}_T|\Lambda &= H(\Lambda) \\ E[\hat{A}_T|\Lambda = \lambda] &= E[A_T|\Lambda = \lambda] \\ \mathrm{var}[\hat{A}_T|\Lambda = \lambda] &= \mathrm{var}[A_T|\Lambda = \lambda] \end{aligned} \tag{4.20}$$

for $\lambda \in (-\infty, \lambda(K))$. Here, $H(\Lambda)$ is a non-negative random variable whose distribution has at least two parameters in order to match the first two moments as stated in Eq. (4.20). In this case, we have

$$\hat{C}_1(T, K, \Lambda, \lambda(K)) = e^{-rT} \int_{-\infty}^{\lambda(K)} E[(H(\lambda) - K)^+] \, f_\Lambda(\lambda) \, \mathrm{d}\lambda. \tag{4.21}$$

It is necessary to calculate the conditional mean and variance of the arithmetic average to determine the corresponding parameters in $H(\lambda)$ for all values of λ. Afterwards, we resort to numerical integration to evaluate the above integral.

Inspired by the work in Curran (1994) and Lord (2006a), we consider an approximation of the arithmetic average by a shifted lognormally distributed variable. This is a convenient choice since the inner expectation in Eq. (4.21) can be calculated by applying the standard Black-Scholes formula, so the evaluation of $\hat{C}_1(T, K, \Lambda, \lambda(K))$ is fairly straightforward. Our numerical experiments reveal that the use of a shifted lognormal approximation in the PEB approximation method does provide sufficient level of accuracy under time-changed Lévy processes already. Recall that $G_T = e^{\ln S_0 + \frac{r-q}{2}T + \Lambda}$ and defining a function

$$g(\lambda) = e^{\ln S_0 + \frac{r-q}{2}T + \lambda},$$

we then construct the following two types of approximations.

1. *Curran 2M+ approximation*

$$\hat{A}_T|\Lambda = H(\Lambda) = G_T + e^{\mu(\Lambda)+\sigma(\Lambda)W}. \tag{4.22a}$$

2. *Curran 3M+ approximation*

$$\hat{A}_T|\Lambda = H(\Lambda) = m_1(G_T) + e^{m_2(\Lambda)+m_3(\Lambda)W}. \tag{4.22b}$$

Here, W is a standard normal random variable. In the 2M+ approximation, $\mu(\Lambda)$ and $\sigma(\Lambda)$ are parameters chosen so as to match the two conditional moments, while $m_1(G_T), m_2(\Lambda)$ and $m_3(\Lambda)$ in the 3M+ approximation are determined such that the three conditional moments are matched exactly. Compared to other PEB approximations, the Curran 2M+ approximation maintains the desirable property that $\hat{A}_T \geq G_T$. The Curran 3M+ approximation sacrifices the satisfaction of $\hat{A}_T \geq G_T$, while the conditional skewness is matched exactly. Since the extra computational effort required in the Curran 3M+ approximation may become too excessive while the Curran 2M+ approximation already yields sufficiently accurate results, we only adopt the Curran 2M+ approximation in our numerical tests. Based on the two conditional moments matching conditions as specified in Eqs. (4.20) and (4.22a), we have the following constraints for the pair of parameters $\mu(\lambda)$ and $\sigma(\lambda)$

$$\begin{aligned} e^{\mu(\lambda)+\frac{1}{2}\sigma^2(\lambda)} &= E[\hat{A}_T - G_T|\Lambda = \lambda] = E[A_T|\Lambda = \lambda] - g(\lambda), \\ e^{2[\mu(\lambda)+\sigma^2(\lambda)]} &= E[\left(\hat{A}_T - G_T\right)^2|\Lambda = \lambda] = E[(A_T - G_T)^2\,|\Lambda = \lambda]. \end{aligned} \tag{4.23}$$

Taking the logarithm of both sides of the above equations and eliminating $\mu(\lambda)$, the volatility term $\sigma(\lambda)$ is given by

$$\sigma(\lambda) = \sqrt{\ln E[(A_T - G_T)^2|\Lambda = \lambda] - 2\ln\left(E[A_T|\Lambda = \lambda] - g(\lambda)\right)},$$

where

$$E[(A_T - G_T)^2\,|\Lambda = \lambda] = \text{var}[A_T|\Lambda = \lambda] + (E[A_T|\Lambda = \lambda])^2 - 2E[A_T|\Lambda = \lambda]g(\lambda) + g^2(\lambda).$$

The conditional expectation and conditional variance of the arithmetic average are given by Eqs. (4.11) and (4.17a), respectively.

For the Curran 2M+ approximation, the inner expectation in Eq. (4.21) can be expressed as a Black-Scholes type European call option price function under the assumption of a shifted lognormally distributed underlying state variable. Here, by assuming $(\hat{A}_T - G_T)|\Lambda = \lambda$ to be a lognormal random variable, we have a new strike price $\hat{K} = K - g(\lambda)$ that is less than the original strike price. The procedure of the Curran 2M+ approximation is summarized in Theorem 5.

Theorem 5 *Based on the Curran 2M+ approximation, the PEB approximation formula for pricing the discrete arithmetic Asian call option is given by*

$$\hat{C}_A(T, K, \Lambda) = \hat{C}_1(T, K, \Lambda, \lambda(K)) + C_2(T, K, \Lambda, \lambda(K)), \tag{4.24}$$

where

$$\begin{aligned} &\hat{C}_1(T, K, \Lambda, \lambda(K)) \\ &= e^{-rT}\int_{-\infty}^{\lambda(K)} \Big[\big(E[A_T|\Lambda = \lambda] - g(\lambda)\big)\Phi(d_1(\lambda)) - \big(K - g(\lambda)\big)\Phi(d_2(\lambda))\Big]\; f_\Lambda(\lambda)\;\mathrm{d}\lambda, \end{aligned} \tag{4.25}$$

and $C_2(T, K, \Lambda, \lambda(K))$ is given by Eq. (3.9), where

$$\begin{aligned} d_1(\lambda) &= \frac{\mu(\lambda) + \sigma^2(\lambda) - \ln\hat{K}}{\sigma(\lambda)} = \frac{\frac{1}{2}\ln E[(A_T - g(\lambda))^2\,|\Lambda = \lambda] - \ln(K - g(\lambda))}{\sigma(\lambda)}, \\ d_2(\lambda) &= d_1(\lambda) - \sigma(\lambda). \end{aligned}$$

When the strike price K approaches to zero, both the bounds and PEB approximation converge to the exact Asian option price. The PEB approximation also tends to the exact Asian option price when K approaches infinity. Recall that the sharp lower bound satisfies this property while the upper bound fails since the bound of the pricing error increases with the strike price K.

Remarks

1. The lower bound $LB(\Lambda)$ and PEB approximation for the discrete arithmetic Asian options can be extended to any models for which the multivariate characteristic functions of the underlying asset price process are known. More specifically, the lower bound only requires the first two types of the following multivariate characteristic functions, while the upper bound or PEB approximation depends on the calculation of all of the following four types of multivariate characteristic functions.

   (a) $\phi_\Lambda(\omega_1) = \phi_Z(\Theta^{(1)})$, where the j^{th} component of $\Theta^{(1)}$ is given by $\theta_j^{(1)} = \frac{\omega_1}{N+1}$, $j = 1, 2, \cdots, N$;

   (b) $\phi_{\Lambda,Z_k}(\omega_1, -i) = \phi_Z(\Theta^{(2)})$, where the components of $\Theta^{(2)}$ are given by $\theta_j^{(2)} = \frac{\omega_1}{N+1}$ for any $j \neq k$, and $\theta_k^{(2)} = \frac{\omega_1}{N+1} - i$;

   (c) $\phi_{\Lambda,Z_k,Z_l}(\omega_1, -i, -i) = \phi_Z(\Theta^{(3)})$, where the components of $\Theta^{(3)}$ are given by $\theta_j^{(3)} = \frac{\omega_1}{N+1}$ for any $j \neq k$ and $j \neq l$, and $\theta_j^{(3)} = \frac{\omega_1}{N+1} - i$ for $j = k$ or $j = l$;

   (d) $\phi_{\Lambda,Z_k}(\omega_1, -2i) = \phi_Z(\Theta^{(4)})$, where the components of $\Theta^{(4)}$ are given by $\theta_j^{(4)} = \frac{\omega_1}{N+1}$ for any $j \neq k$, and $\theta_k^{(4)} = \frac{\omega_1}{N+1} - 2i$.

2. The price of a discrete arithmetic Asian put option

$$P_A(T, K) = e^{-rT} E[(K - A_T)^+]$$

   can be evaluated via the following put-call parity relation

$$P_A(T, K) = C_A(T, K) - e^{-rT} \frac{S_0}{N+1} \frac{1 - e^{(r-q)(N+1)\Delta}}{1 - e^{(r-q)\Delta}} + K e^{-rT}. \tag{4.26}$$

3. Since the Curran 2M+ approximation involves numerical evaluation of triple integrals, we would like to provide some guidelines on how to choose the damping factors, number of integrations points and truncation of computational domain in the actual implementation of the approximation method.

   (a) Damping factors
   We have provided some guidelines on the choice of the damping factor ω_I for calculating the lower bound. One may adopt the same technique shown in Lord and Kahl (2007) to find the optimal damping factor ω_I. Generally, the optimal damping factor should be chosen to ensure that the integrand is neither peaked nor oscillatory. A plot of the integrand with respect to different choices of damping factor may be helpful in searching for the proper damping factor. The same technique can be applied for finding the appropriate damping factors ω_{1I}, ω_{2I} for the Curran 2M+ approximation. The optimal damping factor ω_I also provides a good initial guess for the optimal damping factors ω_{1I}, ω_{2I}.

   Once effective damping factors are chosen, one can achieve the same level of accuracy in the numerical calculation of the integrals using smaller number of discretization grids. In our numerical tests, we chose equal values for the damping factors and adopted $-5, -5, -3.5$ for the Heston model, NIC-CIR process and Kou's model, respectively. These damping factors are shown to provide very accurate and efficient numerical results in our numerical tests.

(b) Truncation of the computational domain
Once the damping factors have been properly chosen, the plot of the corresponding $\widetilde{g}(\omega_1, \omega_2)$ can help determine the truncation ranges for ω_{1R}, ω_{2R}. The function $\widetilde{g}(\omega_1, \omega_2)$ decays to zero as $|\omega_{1R}|$ or $|\omega_{2R}|$ becomes large. We determine the truncation ranges such that the function $\widetilde{g}(\omega_1, \omega_2)$ is smaller than some preset error tolerance provided that ω_{1R} and ω_{2R} do not lie within the truncation ranges. Also, by plotting the integrand in the integral in Eq. (4.25), we can deduce the appropriate truncation range for λ in a similar manner. We did not transform the integrands in our implementation procedure. Alternatively, as inspired by the work of Lord and Kahl (2007), one may avoid the truncation approximation of the infinite domains for calculating the conditional variance by transforming the double infinite integrals into finite domains using the limiting behaviour of the characteristic functions.

(c) Number of integrations points
Let $N_{\omega_1}, N_{\omega_2}, N_\lambda$ denote the number of integration points required for the numerical integration with respect to the variables ω_{1R}, ω_{2R}, and λ, respectively. To achieve a preset discretization error tolerance TOL, we can search for the smallest number of integration points that observes

$$\left|\hat{C}_A(N_{\omega_1}, N_{\omega_2}, N_\lambda) - \hat{C}_A(\infty, \infty, \infty)\right| < TOL.$$

A similar technique has been used in Lord (2006a). As a result, the approximation can exhibit an optimal efficiency for a given discretization error tolerance. We note that the computation cost of the Curran 2M+ approximation is determined by the numerical calculations of the function $\widetilde{g}(\omega_1, \omega_2)$ and the triple integral [in fact dominated by the calculation of $\widetilde{g}(\omega_1, \omega_2)$ in most cases], so the choice of N_λ has a small effect on efficiency of the approximation. As a result, N_λ is not required to be as small as possible, and it is taken to be 2^6 in our numerical tests. For most cases, one may conveniently set $N_{\omega_1} = N_{\omega_2}$, so it is necessary to search for only one parameter for a given TOL. Take our last numerical test as an example, when $T = 5$ and $\sigma = 0.12$, the smallest number of integration points for the PEB approximation (Curran 2M+ approximation) was taken to be 175, that is, $N_{\omega_1} = N_{\omega_2} = 175$.

5 Specification of the activity rate processes

In this section, we show how to derive the explicit representation of I_0 in Eq. (2.10) for some specific choices of the activity rate processes associated with the time change T_t. One popular choice of the activity rate process is the affine process, which nests the well known CIR model. Firstly, we consider absence of the leverage effect, where the base Lévy process is independent of the corresponding activity rate process of the time change. Next, we will demonstrate how to deal with the popular Heston stochastic volatility model, which can be nested in the class of time-changed Lévy processes with the leverage effect. Finally, we give a brief discussion on pricing the discrete arithmetic Asian options under Lévy processes.

5.1 Affine processes as the activity rates

Let U_t be a d-dimensional Markov process that satisfies the following dynamics

$$\mathrm{d}U_t = \tilde{\mu}(U_t)\ \mathrm{d}t + \tilde{\sigma}(U_t)\ \mathrm{d}W_t, \tag{5.1}$$

where W_t is a d-dimensional Brownian motion under Q. The drift vector $\tilde{\mu}(U_t)$ and diffusion covariance matrix $\tilde{\sigma}(U_t)\tilde{\sigma}(U_t)^T$ are affine in U_t, where

$$\tilde{\mu}(U_t) = K_0 + K_1 U_t, \quad K_0 \in \mathbb{C}^d,\ K_1 \in \mathbb{C}^{d\times d}, \tag{5.2a}$$

$$[\tilde{\sigma}(U_t)\tilde{\sigma}(U_t)^T]_{ij} = (H_0)_{ij} + (H_1)_{ij}^T U_t, \quad H_0 \in \mathbb{C}^{d\times d},\ H_1 \in \mathbb{C}^{d\times d\times d}. \tag{5.2b}$$

We require that the vector $\tilde{\mu}(U_t)$ and matrix $\tilde{\sigma}(U_t)$ satisfy some technical conditions such that the stochastic differential equation has a strong solution (Duffie and Kan, 1996). We choose a linear function of the Markov process U_t as the instantaneous activity rate v_t.

Based on the work by Duffie *et al.* (2000) for the affine term structure models, the multivariate characteristic function of the intertemporal joint distribution of $Z = (Z_{t_1}, Z_{t_2}, \cdots, Z_{t_N})$ has been derived by Umezawa and Yamazaki (2015) using Corollary 1. Their results are summarized in Proposition 2.

Proposition 2 *Suppose X_{T_t} follows a time-changed Lévy process under a risk neutral measure Q where an activity rate process v_t is assumed to be*

$$v_t = \rho_0 + \rho_1^T U_t, \quad \textit{for all } t \geq 0, \quad \rho_0 \in \mathbb{C},\ \rho_1 \in \mathbb{C}^d,$$

where U_t is a d-dimensional affine process defined in Eqs. (5.1) and (5.2a, 5.2b). Furthermore, the base Lévy process X_t is assumed to be independent of the activity rate process v_t of the time change. The multivariate characteristic function of the intertemporal joint distribution of Z is given by

$$\phi_Z(\Theta) = e^{\sum_{j=1}^N \alpha_{t_j}(t_{j-1}) + \beta_{t_1}(0)^T U_0},$$

and $\alpha_{t_j} : [t_{j-1}, t_j] \to \mathbb{C}$ and $\beta_{t_j} : [t_{j-1}, t_j] \to \mathbb{C}^d$ are solved recursively by the following complex-valued Riccati differential equations:

$$\frac{\mathrm{d}}{\mathrm{d}t}\beta_{t_j}(t) = \kappa_j \rho_1 - K_1^T \beta_{t_j}(t) - \frac{1}{2}\beta_{t_j}(t)^T H_1 \beta_{t_j}(t), \tag{5.3a}$$

$$\frac{\mathrm{d}}{\mathrm{d}t}\alpha_{t_j}(t) = \kappa_j \rho_0 - K_0^T \beta_{t_j}(t) - \frac{1}{2}\beta_{t_j}(t)^T H_0 \beta_{t_j}(t), \tag{5.3b}$$

with boundary conditions $\alpha_{t_j}(t_j) = 0$ for $j = 1, \cdots, N$, $\beta_{t_N}(t_N) = 0$ and $\beta_{t_j}(t_j) = \beta_{t_{j+1}}(t_j)$ for $j = 1, \cdots, N-1$. Here, $\kappa_j = \psi_X(\sum_{k=j}^N \theta_k) - i(\sum_{k=j}^N \theta_k)\psi_X(-i)$.

5.2 Heston stochastic volatility model

Under the Heston stochastic volatility model, the correlated stochastic processes S_t and v_t with correlation coefficient ρ under a risk neutral measure Q are governed by

$$\frac{\mathrm{d}S_t}{S_t} = (r-q)\ \mathrm{d}t + \sqrt{v_t}\ \mathrm{d}W_t^1, \tag{5.4}$$

$$\mathrm{d}v_t = \zeta(\bar{v} - v_t)\ \mathrm{d}t + \sigma_v\sqrt{v_t}\left(\rho\ \mathrm{d}W_t^1 + \sqrt{1-\rho^2}\ \mathrm{d}W_t^2\right). \tag{5.5}$$

The asset return S_t can be expressed as a time-changed Lévy process with the leverage effect specified as

$$S_t = S_0 e^{(r-q)t + X_{T_t} - \frac{1}{2}T_t},$$

where the corresponding base Lévy process $X_t = W_t^1$. We define the new complex-valued measure $Q(\theta)$ by the following exponential martingale

$$\mathbb{M}_t(\theta) = e^{i\theta \int_0^t \sqrt{v_s} \ \mathrm{d}W_s^1 + \frac{1}{2}\theta^2 \int_0^t v_s \ \mathrm{d}s}.$$

Applying the Girsanov theorem, the activity rate v_t under $Q(\theta)$ measure is governed by the following stochastic differential equation

$$\mathrm{d}v_t = [\zeta\bar{v} - (\zeta - i\theta\sigma_v\rho)v_t]\,\mathrm{d}t + \sigma_v\sqrt{v_t}\left(\rho \ \mathrm{d}W_t^\theta + \sqrt{1-\rho^2} \ \mathrm{d}W_t^2\right),$$

where $\mathrm{d}W_t^\theta = \mathrm{d}W_t^1 - i\theta\sqrt{v_t}\,\mathrm{d}t$ is a Brownian motion under $Q(\theta)$. Good analytical tractability is retained since v_t remains to be an affine process under the new complex-valued measure $Q(\theta)$. According to Eq. (2.9), it is necessary to change measure at each time step when the correlation is incorporated, which is cumbersome. Fortunately, we manage to obtain the multivariate characteristic function of the joint distribution under the Heston stochastic volatility model by following a similar technique in Proposition 2.

Proposition 3 *Suppose the asset return follows the Heston stochastic volatility model as governed by Eqs. (5.4) and (5.5). The multivariate characteristic function of the intertemporal joint distribution of Z is given by*

$$\phi_Z(\Theta) = e^{\sum_{j=1}^N \alpha_{t_j}(t_{j-1}) + \beta_{t_1}(0)v_0},$$

where $\alpha_{t_j} : [t_{j-1}, t_j] \to \mathbb{C}$ and $\beta_{t_j} : [t_{j-1}, t_j] \to \mathbb{C}$ are solved recursively by the following complex-valued Riccati differential equations:

$$\frac{\mathrm{d}}{\mathrm{d}t}\beta_{t_j}(t) = \kappa_j + \left[\zeta - i\Big(\sum_{k=j}^N \theta_k\Big)\sigma_v\rho\right]\beta_{t_j}(t) - \frac{1}{2}\sigma_v^2\beta_{t_j}(t)^2, \tag{5.6a}$$

$$\frac{\mathrm{d}}{\mathrm{d}t}\alpha_{t_j}(t) = -\zeta\bar{v}\beta_{t_j}(t), \tag{5.6b}$$

with boundary conditions: $\alpha_{t_j}(t_j) = 0$ for $j = 1, \cdots, N$, $\beta_{t_N}(t_N) = 0$, $\beta_{t_j}(t_j) = \beta_{t_{j+1}}(t_j)$ for $j = 1, \cdots, N-1$; and

$$\kappa_j = \frac{1}{2}\left[\Big(\sum_{k=j}^N \theta_k\Big)^2 + i\Big(\sum_{k=j}^N \theta_k\Big)\right]. \tag{5.7}$$

In Appendix B, we present the closed form solutions for the above complex-valued Riccati differential equations. Suppose the activity rate v_t of a time-changed Lévy process X_{T_t} is also given by Eq. (5.5) and it is independent of the corresponding base Lévy process X_t, by replacing $\rho = 0$ and $\kappa_j = \psi_X(\sum_{k=j}^N \theta_k) - i(\sum_{k=j}^N \theta_k)\psi_X(-i)$, we can derive the multivariate characteristic function of the intertemporal joint distribution of time-changed Lévy processes with zero correlation.

5.3 Lévy processes

Note that a general Lévy process is a reduced form of the time-changed Lévy process by choosing the constant activity rate $v_t = 1$. The bounds and approximations derived in the above sections for pricing discrete arithmetic Asian options under time-changed Lévy processes are also applicable for Lévy processes. According to Eq. (2.11), the closed form for the multivariate characteristic function of the intertemporal joint distribution of Lévy processes are presented in Proposition 4.

Proposition 4 *Suppose $T_t = t$ for all $t \geq 0$, a time-changed Lévy process X_{T_t} is reduced to a Lévy process X_t. The multivariate characteristic function of the intertemporal joint distribution of Z is given by*

$$\phi_Z(\Theta) = e^{-\sum_{j=1}^{N}[\psi_X(\sum_{k=j}^{N}\theta_k) - i(\sum_{k=j}^{N}\theta_k)\psi_X(-i)]\Delta}. \tag{5.8}$$

6 Numerical tests on various pricing bounds and approximations

In this section, we would like to demonstrate the performance of the various types of approximation formulas for pricing discrete arithmetic Asian call options under the Heston stochastic volatility model, NIG-CIR model and Kou's model. Here, the NIG-CIR model refers to the time-changed Lévy process with the Normal Inverse Gaussian process as the base Lévy process and the CIR process as an activity rate process of the time change. The parameter values in the time-changed Lévy models are chosen from earlier papers so that direct comparison with other methods in the literature can be performed. The Gauss-Legendre quadrature rule is adopted to evaluate the integrals in the pricing formulas. Compared to the composite trapezodial rule, the Gauss-Legendre quadrature rule exhibits faster rate of convergence with respect to the number of the grids chosen in the numerical integration. It is observed that numerical accuracy in the valuation of the analytic pricing formulas is not sensitive to the choice of the quadrature rule.

6.1 Time-changed Lévy processes

The characteristic exponent of the Normal Inverse Gaussian process (NIG) is given by

$$\psi_X(\xi) = \frac{1}{\hat{k}} \ln\left(1 + \frac{\hat{k}\sigma^2\xi^2}{2} - i\hat{\mu}\hat{k}\xi\right). \tag{6.1}$$

The CIR process as defined in Eq. (5.5) is chosen to be the activity rate for the time-changed Lévy process. We assume the NIG process to be independent of the corresponding CIR process. On the other hand, we consider a leverage effect in the Heston model. In order to perform direct comparison with the Gram-Charlier expansion proposed by Yamazaki (2014), we consider a slightly modified definition of the arithmetic average $A_T = \frac{1}{N}\sum_{k=1}^{N} S_{t_k}$ in this subsection. In our calculations, we take $S_0 = 100,\ T = 1,\ N = 10,\ r = 0.01$, and $q = 0.02$ in the discrete arithmetic Asian call option. The parameter values for the two time-changed Lévy processes, the Heston model and NIG-CIR model, are taken from Yamazaki (2014) and they are listed in Table 1.

		Heston	NIG-CIR
Lévy processes	σ	1.00	0.10
	$\hat{\mu}$	-	-0.50
	$\hat{k}$	-	0.01
CIR process	ζ	1.00	1.00
	$\bar{v}$	0.01	1.00
	σ_v	0.10	1.00
	ρ	-0.70	0.00
	v_0	0.01	1.00

Table 1: Parameter values of the Heston model and NIG-CIR model.

It is shown in Yamazaki (2014) that approximating the infinite series with sum of a small number of terms using the Gram-Charlier expansion might not be sufficient to obtain accurate values in practice due to higher kurtosis generated by stochastic time change and jumps. His numerical tests show that summing seven terms is required to achieve sufficiently accurate prices of Asian call options. We would like to compare our numerical results with those obtained by the Gram-Charlier expansion method. The numerical option values obtained from the Monte Carlo simulation with 500 time steps and 10 million sample paths are used as benchmark. Tables 2 and 3 list the numerical results obtained by using the lower and upper bounds and PEB approximation together with the benchmark Monte Carlo method for pricing discrete arithmetic Asian call options with varying values of K under the Heston stochastic volatility model and NIG-CIR model, respectively.

K	90	95	100	105	110
Monte Carlo	9.590	5.307	2.120	0.491	0.051
Standard error(10^{-3})	1.74	1.50	0.97	0.44	0.13
Gram-Charlier	9.582	5.307	2.118	0.488	0.049
Lower bound	9.5852	5.3034	2.1173	0.4890	0.0499
PEB (Curran 2M+)	9.5853	5.3035	2.1173	0.4890	0.0499
Upper bound	9.5914	5.3165	2.1379	0.5161	0.0810

Table 2: Comparison of various approximations of the discrete arithmetic Asian option prices under the Heston model. Numerical results from Monte Carlo simulation (with small standard errors) are provided for benchmark comparison.

K	90	95	100	105	110
Monte Carlo	9.610	5.430	2.410	0.812	0.215
Standard error(10^{-3})	1.99	1.70	1.22	0.72	0.37
Gram-Charlier	9.614	5.430	2.407	0.808	0.216
Lower bound	9.6113	5.4299	2.4092	0.8108	0.2144
PEB (Curran 2M+)	9.6115	5.4301	2.4093	0.8109	0.2145
Upper bound	9.6184	5.4457	2.4345	0.8445	0.2542

Table 3: Comparison of various approximations of the discrete arithmetic Asian option prices under the NIG-CIR model. Numerical results from Monte Carlo simulation (with small standard errors) are provided for benchmark comparison.

As revealed from Tables 2 and 3, the PEB approximation (Curran 2M+ approximation) and the lower bound perform very well in numerical accuracy and exhibit slightly better accuracy than the Gram-Charlier expansion method. The PEB approximation values lie between the sharp lower bound and the upper bound, an observation that is consistent with the theoretical analysis. Indeed, accuracy of the PEB approximation can be gauged by the difference between the upper bound and the lower bound, while the pricing errors using the Gram-Charlier expansion method have to be accessed via additional numerical studies. It is highly computationally efficient to evaluate the lower bound with good accuracy. For example, it only took 0.11 seconds to obtain the value 2.4092 for the lower bound when the strike equals 100 under the NIG-CIR process in our calculations. The computational efforts involved in the calculations of the PEB approximation and upper bound are more demanding since the calculation of the conditional variance is also required and the pricing formulas involve triple integrations. For example, 0.72 seconds are required to obtain the numerical value 2.4093 using the PEB approximation. Less computational time is required when we choose to loosen accuracy requirement for the bounds and approximation. The upper bound is in general less accurate than the lower bound. The numerical results show that the difference between the upper bound and lower bound is an increasing function of the strike price K. For both at-the-money and in-the-money options, the upper bound results are fairly accurate for the discrete arithmetic Asian call options. However, the results for out-of-the-money options are slightly less accurate. Finally, when the Asian option is sufficiently deep in-the-money, both the bounds and the PEB approximation converge to the Asian call option price.

Albrecher *et al.* (2008) give model independent lower bounds for discrete arithmetic Asian option prices. Instead of conditioning on the geometric average variable, they choose S_t as the conditioning variable to achieve a robust bound. They derive the corresponding lower bounds $LB_t^{(1)}$ and $LB_t^{(2)}$ based on the following assumptions on stop-loss orders

$$A_T \geq_{sl} \frac{1}{N}\left(\sum_{i=1}^{j(t)-1} S_0 e^{rt_i} + \sum_{i=j(t)}^{N} S_t e^{r(t_i-t)}\right) \tag{6.2a}$$

and

$$A_T \geq_{sl} \frac{1}{N}\left(\sum_{i=1}^{j(t)-1} S_0^{1-\frac{t_i}{t}} S_t^{\frac{t_i}{t}} + \sum_{i=j(t)}^{N} S_t e^{r(t_i-t)}\right), \tag{6.2b}$$

respectively, where $j(t) = \min\{i : t_i \geq t\}$ for any $0 \leq t \leq T$. The stop-loss order $\geq_{sl}$ of two random variables is defined by

$$X \geq_{sl} Y \Leftrightarrow E[(X-d)^+] \geq E[(Y-d)^+], \quad -\infty < d < \infty. \tag{6.3}$$

It is easily seen that the stop-loss order is weaker than the convex order. Albrecher *et al.* (2008) computed the bounds for discrete arithmetic Asian option prices under the Heston stochastic volatility model using the following parameters

$$\zeta = 1.5768,\ \bar{v} = 0.0398,\ \sigma_v = 0.5751,\ \rho = -0.5711,\ \text{and } v_0 = 0.0175.$$

Note that the lower bound $LB(\Lambda)$ also works for any asset price process, provided that the multivariate characteristic functions are known in closed form. Figure 1 shows the comparison of different lower bounds for the arithmetic Asian call option prices under the Heston stochastic volatility model. As revealed from Figure 1, the lower bounds provided by $LB_t^{(1)}$ and $LB_t^{(2)}$ are seen to be less accurate when compared to $LB(\Lambda)$, indicating that the geometric average is a better conditioning variable compared to S_t.

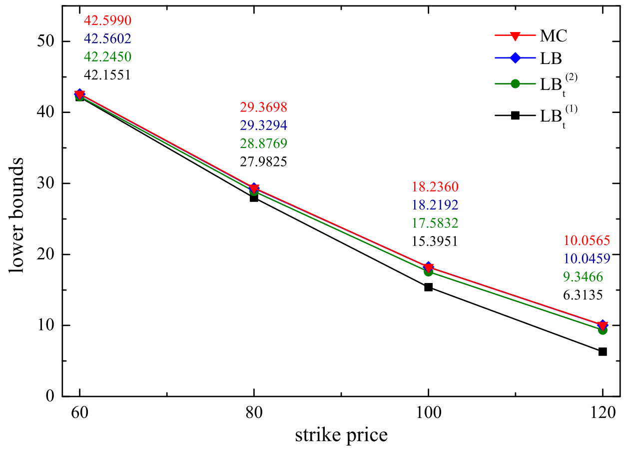

Figure 1: Comparison of various lower bounds of the discrete arithmetic Asian call option prices under the Heston stochastic volatility model with $r = 0.03,\ q = 0,\ S_0 = 100,\ T = 10$ and monthly averaging. The benchmark results are obtained using the Monte Carlo method with 10^6 simulation paths.

6.2 Lévy processes

Next, we would like to show that the sharp lower bound and PEB approximation also perform well for pricing discrete arithmetic Asian options under Lévy processes. The time-changed Lévy process is reduced to a Lévy process by choosing a constant activity rate $v_t = 1$. Fusai and Meucci (2008) adopt the numerical quadrature (NQ) for a recursive convolution algorithm to price discrete arithmetic Asian options under Lévy processes. In another work, Fusai *et al.* (2011) extend the maturity randomization technique to price discrete arithmetic Asian options under Lévy processes. Zhang and Oosterlee (2013) propose an efficient pricing method for discrete arithmetic Asian options based on the Fourier cosine expansions and Clenshaw-Curtis quadrature. Note that all these methods are convolution methods, which rely on the independent increments of the log-asset returns. Therefore, they cannot be used for pricing Asian options under time-changed Lévy processes.

To demonstrate the numerical performance of the PEB approximation, lower and upper bound under Lévy processes, we performed the numerical calculations of the discrete Asian call options under Kou's model as a prototype. The characteristic exponent of Kou's model is given by

$$\psi_X(\xi) = \frac{\sigma^2}{2}\xi^2 - \hat{\lambda}\left[\frac{(1-p)\eta_2}{\eta_2 + i\xi} + \frac{p\eta_1}{\eta_1 - i\xi} - 1\right], \tag{6.4}$$

where σ is the volatility for the diffusion part, $\hat{\lambda}$ is the jump intensity for the Poisson process, p and $1-p$ are the respective probability of up-jump and down-jump, η_1 and η_2 are the respective up and down jump sizes for the exponential distribution. The parameter values for the discrete arithmetic Asian call options used in our sample calculations are listed in Table 4. These parameter values in Kou's model are taken from the same set of parameter values obtained in Schoutens (2003) based on their calibration to the $S\&P$ 500 option prices.

S_0	T	r	q	σ	$\hat{\lambda}$	p	η_1	η_2
100	1	0.0367	0	0.120381	0.330966	0.2071	9.65997	3.13868

Table 4: Parameter values for the discrete arithmetic Asian call option under Kou's model.

In Table 5, we show the comparison of numerical accuracy of the PEB approximation with other approximation methods in the literature. The numerical option values obtained from the Monte Carlo simulation with one million simulation paths are used as the benchmark and the standard errors (SE) are provided (see the last column in Table 5). The PEB approximation (Curran 2M+ approximation) values agree very well with the Monte Carlo results. In most cases, they are more accurate than the values for the lower bound. The results obtained by Fusai and Meucci (2008) and Fusai *et al.* (2011) agree with those of the PEB approximation up to three-decimal accuracy.

N	K	PEB	LB	NQ	UB	MC	SE$_{(10^{-3})}$
12	90	12.71331	12.70817	12.71236	12.82116	12.71298	0.374
12	100	5.01825	5.01609	5.01712	5.18227	5.01729	0.238
50	100	5.05934	5.05717	5.05809	5.22421	5.05849	0.241
50	110	1.06906	1.06829	1.06878	1.27688	1.06886	0.189
250	100	5.07068	5.06851	5.06949	5.23581	5.06910	0.245
250	110	1.07672	1.07595	1.07646	1.28460	1.07632	0.191

Table 5: Numerical prices of the discrete arithmetic Asian options under Kou's model with $N = 12, N = 50$, and $N = 250$ (monthly, weekly, and daily monitored, respectively) obtained from the numerical calculations of the lower bound (LB), upper bound (UB) and PEB approximation (Curran 2M+ approximation). These numerical results are compared with numerical prices obtained by the numerical quadrature (NQ) method and Monte Carlo (MC) method listed in Fusai and Meucci (2008). The last column (SE) lists the standard errors in the Monte Carlo simulation.

We performed another set of numerical tests to reveal more closely the issue of numerical accuracy/computational effort tradeoff between the PEB approximation and lower bound method by considering varying values of maturity and volatility of the diffusion part of Kou's model. Recall that the lower bound and the PEB approximation (Curran 2M+ approximation) are evaluated based on numerical integration, we searched for the smallest number of integration points such that the corresponding discretization errors are smaller than 1×10^{-5} (i.e. $TOL = 10^{-5}$) in our numerical tests. One can then proceed to compare the CPU times for the lower bound and the PEB approximation in a relatively fair manner. A similar technique of comparing numerical accuracy/CPU time has been used in Lord (2006a). The numerical results and the CPU times required for computing the lower bound and PEB approximation for Asian option prices with yearly averaging are displayed in Table 6. Given the same discretization error tolerance ($TOL = 10^{-5}$), the lower bound converges quite fast but retains a fixed level of numerical error afterwards. On the other hand, the PEB approximation achieves high level of numerical accuracy while the CPU times required for the PEB calculations are acceptable. The CPU times required for calculating the PEB approximation values are typically 10 to 40 times those for calculating the lower bound values. If we demand for high level of accuracy for long maturity Asian option prices while the computational budget is not too restrictive, then the PEB approximation has comparable advantage over the lower bound method.

σ	T	PEB (CPU)	LB (CPU)	MC	SE	EP	EL
0.12	5	14.2456 (0.13)	14.2280 (0.01)	14.2461	0.0013	-0.0005	-0.0181
	10	21.2031 (0.25)	21.1699 (0.01)	21.2019	0.0027	0.0012	-0.0320
	15	25.7053 (0.36)	25.6610 (0.02)	25.7057	0.0045	-0.0004	-0.0447
	20	28.7074 (0.63)	28.6556 (0.02)	28.7066	0.0064	0.0008	-0.0510
0.3	5	19.6025 (0.13)	19.5661 (0.01)	19.6081	0.0046	-0.0056	-0.0420
	10	27.3593 (0.34)	27.2862 (0.01)	27.3603	0.0049	-0.0010	-0.0741
0.5	5	26.8766 (0.18)	26.7802 (0.01)	26.8783	0.0068	-0.0017	-0.0981

Table 6: Comparison of numerical accuracy and CPU times (in seconds) of the lower bound and the PEB approximation (Curran 2M+ approximation) for computing at-the-money Asian option prices with yearly averaging for varying values of maturity T and volatility σ. The pricing errors of the PEB approximation (EP) and those of the lower bound (EL) are listed in the last two columns.

As a final remark, our numerical tests reveal that the PEB approximation and lower bound perform well in numerical accuracy and computational efficiency when we consider pricing discrete arithmetic Asian options under Lévy processes. Unlike the convolution methods, which can be used for pricing discrete arithmetic Asian options under asset price process with the independent increments property, the PEB approximation method and lower bound are applicable to a wider class of asset price processes.

7 Conclusion

We derive analytical lower and upper bounds for pricing discrete arithmetic Asian options under time-changed Lévy processes. Calculation of the option delta can be performed without additional computation efforts. We also present the class of partially exact and bounded (PEB) approximations, which can produce highly accurate approximations and lie between a sharp lower bound and an upper bound. Indeed, the sharp lower bound obtained by Jensen's inequality can be considered as an element of this class of approximations. Thanks to Umezawa and Yamazaki (2015) on the explicit analytic forms of the multivariate characteristic function of the intertemporal joint distribution of time-changed Lévy processes, we extend the previous work for pricing bounds (Lemmens *et al.*, 2010) in the Lévy setting to the general time-changed Lévy processes. The class of the PEB approximations introduced by Lord (2006a) under the Geometric Brownian motion for the underlying price process have been generalized to time-changed Lévy processes, allowing for jumps, stochastic volatility, and mean reversion. The PEB approximations are more widely applicable to asset price processes for pricing discrete arithmetic Asian option than other approximation methods proposed in the existing literature.

Numerical tests demonstrate that the class of PEB approximations can achieve accurate, efficient and reliable approximations for pricing discrete arithmetic Asian options under the Heston stochastic volatility model, NIG-CIR model and Kou's model. The PEB approximations converge to the exact Asian option price when the strike price approaches to zero or infinity. Though the upper bound is less accurate and efficient than the lower bound, it is significantly more accurate than the comonotonic upper bound.

One may be concerned with the numerical challenge and computational tediousness in the calculations of the upper bound and the PEB approximation for discrete arithmetic Asian options under time-changed Lévy processes since the calculation of the conditional variance is required as part of the computational procedure. With regard to computational efficiency, our numerical experiments show that when an effective damping factor in the numerical Fourier inversion procedure is chosen, the computational time required to achieve a high level of numerical accuracy for the PEB approximation is about 10 to 40 times that of the lower bound calculation for pricing discrete arithmetic Asian options under time-changed Lévy processes. The magnitude of the computational time multiplier is dependent on the number of the monitoring dates.

Acknowledgement

The second author would like to thank the support from the Austrian Science Fund (FWF) under grant P25815 and the European Research Council (ERC) under grant FA506041.

REFERENCES

Albrecher, H., Dhaene, J., Goovaerts, M., and Schoutens, W. (2005). Static hedging of Asian options under Lévy models. *Journal of Derivatives*, **12(3)**, 63-72.

Albrecher, H., Mayer, P., and Schoutens, W. (2008). General lower bounds for arithmetic Asian option prices. *Applied Mathematical Finance*, **15(2)**, 123-149.

Andreasen, J. (1998). The pricing of discretely sampled Asian and lookback options: a change of numeraire approach. *Journal of Computational Finance*, **2(1)**, 5-30.

Benhamou, E. (2000). Fast Fourier transform for discrete Asian options. *Journal of Computational Finance*, **6(1)**, 49-68.

Caldana, R., and Fusai, G. (2013). A general closed-form spread option pricing formula. *Journal of Banking* & *Finance*, **37(12)**, 4893-4906.

Caldana, R., Fusai, G., Gnoatto, A., and Grasselli, M. (2014). General closed-form basket option pricing bounds. Available at SSRN 2376134.

Carr, P., and Wu, L. (2004). Time-changed Lévy processes and option pricing. *Journal of Financial Economics*, **71**, 113-141.

Carverhill, A., and Clewlow, L. (1990). Flexible convolution: valuing average rate (Asian) options. *Risk*, **4(3)**, 25-29.

Clark, P.K. (1973). A subordinated stochastic process model with finite variance for speculative prices. *Econometrica: Journal of the Econometric Society*, **41**, 135-155.

Curran, M. (1992). Beyond average intelligence. *Risk Magazine*, **5(10)**, 60.

Curran, M. (1994). Valuing Asian and portfolio options by conditioning on the geometric mean price. *Management Science*, **40(12)**, 1705-1711.

Duffie, D., and Kan, R. (1996). A yield-factor model of interest rates. *Mathematical finance*, **6(4)**, 379-406.

Duffie, D., Pan, J., and Singleton, K. (2000). Transform analysis and asset pricing for affine jump-diffusions. *Econometrica*, **68(6)**, 1343-1376.

Eberlein, E., and Papapantoleon, A. (2005). Equivalence of floating and fixed strike Asian and lookback options. *Stochastic Processes and their Applications*, **115(1)**, 31-40.

Fusai, G., Marazzina, D., and Marena, M. (2011). Pricing discretely monitored Asian options by maturity randomization. *SIAM Journal on Financial Mathematics*, **2(1)**, 383-403.

Fusai, G., and Meucci, A. (2008). Pricing discretely monitored Asian options under Lévy processes. *Journal of Banking Finance*, **32(10)**, 2076-2088.

Geman, H., and Yor, M. (1993). Bessel processes, Asian options, and perpetuities. *Mathematical Finance*, **3(4)**, 349-375.

Hull, J., and White, A. (1993). Efficient procedures for valuing European and American path-dependent options. *Journal of Derivatives*, **1(1)**, 21-31.

Itkin, A., and Carr, P. (2010). Pricing swaps and options on quadratic variation under stochastic time change models - discrete observations case. *Review of Derivatives Research*, **13**, 141-176.

Lemmens, D., Liang, L.Z.J., Tempere, J., and De Schepper, A. (2010). Pricing bounds for discrete arithmetic Asian options under Lévy models. *Physica A: Statistical Mechanics and its Applications*, **389(22)**, 5193–5207.

Levy, E. (1992). Pricing European average rate currency options. *Journal of International Money and Finance*, **11(5)**, 474-491.

Lord, R. (2006a). Partially exact and bounded approximations for arithmetic Asian options. *Journal of Computational Finance*, **10(2)**, 1-52.

Lord, R. (2006b). Pricing of baskets, Asian and swaptions in general models. *Presentation at the* 5^{th} *Winter school on Financial Mathematics*, available at http://staff.science.uva.nl/∼spr eil/stieltjes/lord.pdf.

Lord, R., and Kahl, C. (2007). Optimal Fourier inversion in semi-analytical option pricing. *Journal of Computational Finance*, **10(4)**, 1-30.

Nielsen, J.A., and Sandmann, K. (2003). Pricing bounds on Asian options. *Journal of Financial and Quantitative Analysis*, **38(2)**, 449-473.

Rogers, L.C.G., and Shi, Z. (1995). The value of an Asian option. *Journal of Applied Probability*, **32(4)**, 1077-1088.

Sato, K.I. (1999). Lévy Process and Infinitely Divisible Distributions. *Cambridge University Press, Cambridge, UK.*

Simon, S., Goovaerts, M.J., and Dhaene, J. (2000). An easy computable upper bound for the price of an arithmetic Asian option. *Insurance: Mathematics and Economics*, **26(2)**, 175-184.

Turnbull, S., McLean, S., and Wakeman, L.M. (1991). Quick algorithm for pricing European average options. *Journal of Financial and Quantitative Analysis*, **26(3)**, 377-389.

Umezawa, U., and Yamazaki, A. (2015). Pricing path-dependent options with discrete monitoring under time-changed Lévy processes. *Applied Mathematical Finance*, **22(2)**, 133-161.

Vanmaele, M., Deelstra, G., Liinev, J., Dhaene, J., and Goovaerts, M.J. (2006). Bounds for the price of discretely sampled arithmetic Asian options. *Journal of Computational and Applied Mathematics*, **185(1)**, 51-90.

Vecer, J. (2000). A new PDE approach for pricing arithmetic average Asian options. *Journal of Computational Finance*, **4(4)**, 105-113.

Wu, L.R. (2008). Modeling financial security returns using Lévy processes. *Handbooks in Operations Research and Management Science*, **15**, 117-162.

Yamazaki, A. (2014). Pricing average options under time-changed Lévy processes. *Review of Derivatives Research*, **17(1)**, 79-111.

Zeng, P., and Kwok, Y.K. (2014). Pricing barrier and Bermudan style options under time-changed Lévy processes: fast Hilbert transform approach. *SIAM Journal on Scientific Computing*, **36(3)**, B450-B485.

Zhang, B., and Oosterlee, C.W. (2013). Efficient pricing of European-style Asian options under exponential Lévy processes based on Fourier cosine expansions. *SIAM Journal on Financial Mathematics*, **4(1)**, 399-426.

Appendix A. Numerical verification of the conditions in Theorem 2

We would like to demonstrate that the sufficient condition in Theorem 2 is satisfied under general time-changed Lévy processes through numerical tests. We have tested a variety of models with different sets of parameter values. Here, we adopt the NIG-CIR process and Kou's model as illustrative examples.

Kou's model
Figure 2 shows that the conditional expectation $E[A_T|\Lambda = \lambda]$ is a monotonically increasing function with respect to λ under Kou's model. One can easily find a unique root λ^* that is close to $\lambda(K)$ for the equation $E[A_T|\Lambda = \lambda] - K = 0$. Note that $G_T = S_0 e^{\frac{r-q}{2}T+\Lambda}$, so with an increase in the geometric average, the expectation of arithmetic average conditional on geometric average increases monotonically.

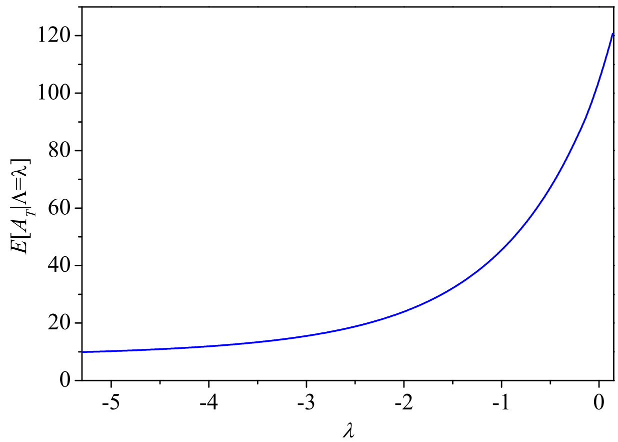

Figure 2: Plot of the conditional expectation $E[A_T|\Lambda = \lambda]$ versus λ under Kou's model.

NIG-CIR process
Figure 3 plots the derivative function $\frac{\mathrm{d}LB_\lambda(\Lambda)}{\mathrm{d}\lambda}$ against the parameter λ under the NIG-CIR process. A similar and typical shape is observed for other time-changed Lévy processes. As revealed in Figure 3, when λ increases, $\frac{\mathrm{d}LB_\lambda(\Lambda)}{\mathrm{d}\lambda}$ only changes its sign at a unique point λ^* and stays negative afterwards. This immediately leads to the result that $\mathcal{S} = [\lambda^*, \infty)$. One may explain this phenomenon via the following intuitive arguments. It is worth mentioning that $\frac{\mathrm{d}LB_\lambda(\Lambda)}{\mathrm{d}\lambda} = -e^{-rT}(E[A_T|\Lambda = \lambda] - K)f_\Lambda(\lambda)$. When λ is very small, the density function $f_\Lambda(\lambda)$ makes the left side of tail of $\frac{\mathrm{d}LB_\lambda(\Lambda)}{\mathrm{d}\lambda}$ decays to zero from above. As λ grows gradually until to $\lambda(K)$, the corresponding geometric average G_T increases at a higher rate and hits the strike price K eventually. Since A_T and G_T are strongly correlated and $A_T \geq G_T$, one may expect that $E[A_T|\Lambda = \lambda]$ starts from a small value and eventually overshoots K. As a result, $\frac{\mathrm{d}LB_\lambda(\Lambda)}{\mathrm{d}\lambda}$ changes its sign within this interval. Once λ crosses $\lambda(K)$, $E[A_T|\Lambda = \lambda]$ remains above K and $\frac{\mathrm{d}LB_\lambda(\Lambda)}{\mathrm{d}\lambda}$ stays negative. As λ increases further, the right tail of $\frac{\mathrm{d}LB_\lambda(\Lambda)}{\mathrm{d}\lambda}$ decays to zero from below.

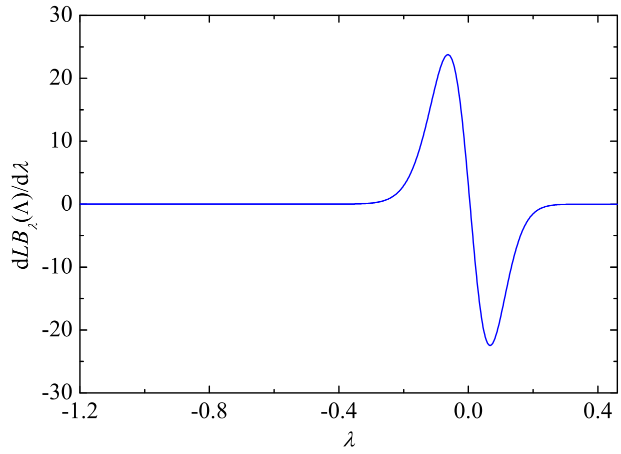

Figure 3: Plot of the derivative function $\frac{\mathrm{d}LB_\lambda(\Lambda)}{\mathrm{d}\lambda}$ versus λ under the NIG-CIR process. When $\lambda \in [-1.2, -0.4]$, $\frac{\mathrm{d}LB_\lambda(\Lambda)}{\mathrm{d}\lambda}$ has very small positive value.

Appendix B. Closed form solutions for the complex-valued Riccati differential equations (see Proposition 3)

Yamazaki (2014) derives the closed form solutions for the complex-valued Riccati differential equations by solving Eqs. (5.6a, 5.6b) when $\kappa_j \neq 0$. Here, we also solve the complex-valued Riccati differential equations when $\kappa_j = 0$. The closed form solutions for the complex-valued Riccati differential equations under $\kappa_j \neq 0$ and $\kappa_j = 0$ are presented below.

1. $\kappa_j \neq 0$
   To present the closed form solutions for the complex-valued Riccati differential equations, we define

$$
\begin{aligned}
B_j &= \zeta - i\Big(\sum_{k=j}^{N}\theta_k\Big)\sigma_v\rho, \quad C_j = \frac{1}{2}\sqrt{B_j^2 + 2\sigma_v^2\kappa_j}, \\
D_j &= -\frac{1}{2\sigma_v^2\kappa_j C_j}\left(\frac{1}{2}B_j + C_j\right)\left[B_j - 2C_j - \sigma_v^2\beta_{t_{j+1}}(t_j)\right], \\
E_j &= -\frac{\sigma_v^2\beta_{t_{j+1}}(t_j)}{B_j - 2C_j}, \quad F_j = -\sigma_v^2\kappa_j D_j, \quad G_j = -\frac{1}{2}\sigma_v^2\beta_{t_{j+1}}(t_j).
\end{aligned}
$$

   For $j = N, N-1, \cdots, 1$, we have

$$
\beta_{t_j}(t) = \frac{2p'_{t_j}(t)}{\sigma_v^2 p_{t_j}(t)} \quad \text{and} \quad \alpha_{t_j}(t) = -\frac{2\zeta\bar{v}}{\sigma_v^2}\ln|p_{t_j}(t)| \tag{B.1}
$$

   for any $t_{j-1} \leq t \leq t_j$, where

$$
\begin{aligned}
p_{t_j}(t) &= D_j e^{-\frac{1}{2}B_j(t_j-t)}\left[B_j\sinh\left(C_j(t_j-t)\right) + 2C_j\cosh\left(C_j(t_j-t)\right)\right] - E_j e^{-(\frac{1}{2}B_j - C_j)(t_j-t)}, \\
p'_{t_j}(t) &= F_j e^{-\frac{1}{2}B_j(t_j-t)}\sinh\left(C_j(t_j-t)\right) - G_j e^{-(\frac{1}{2}B_j - C_j)(t_j-t)}.
\end{aligned}
$$

2. $\kappa_j = 0$
   For $j = N, N-1, \cdots, 1$, we have

$$
\beta_{t_j}(t) = \frac{2p'_{t_j}(t)}{\sigma_v^2 p_{t_j}(t)} \quad \text{and} \quad \alpha_{t_j}(t) = -\frac{2\zeta\bar{v}}{\sigma_v^2}\ln|p_{t_j}(t)| \tag{B.2}
$$

for any $t_{j-1} \leq t \leq t_j$, where

$$p_{t_j}(t) = \frac{\sigma_v^2 \beta_{t_{j+1}}(t_j)}{2B_j} e^{-B_j(t_j - t)} + \frac{2B_j - \sigma_v^2 \beta_{t_{j+1}}(t_j)}{2B_j},$$
$$p_{t_j}^{'}(t) = \frac{1}{2} \sigma_v^2 \beta_{t_{j+1}}(t_j) e^{-B_j(t_j - t)}.$$